C.P. No. 661 C.P. No. 661

MINISTRY OF AVIATION

AERONAUTICAL RESEARCH COUNCIL

CURRENT PAPERS

The Influence of a Wide Hub on the Room Temperature Burst Strength of Model Steam Turbine Rotors

By

N.E. Waldren and D.E. Ward

LONDON: HER MAJESTY'S STATIONERY OFFICE

1963

PRICE 10s 6d NET

U.D.C. No. 531.25-434.3:620.172

C.P. No.661

March 1963

The influence of a wide hub on the room temperature burst strength of model steam turbine rotors

- by -

N. E. Waldren and D. E. Ward

SUMMARY

A number of model steam turbine rotors in various materials has been spun to burst with the object of studying the influence of increased hub width on rotor strength.

Analysis of results shows that substantial strain in the mid-bore region is the result of a compressive stress which, although improving the ductility of the material, can produce local plastic deformation at low rotor speeds. Failure in the rotors has been caused by a high ratio of biaxial tension near the rim and some changes in design are suggested to reduce this ratio, which severely limits the ductility of the material.

Replaces N.G.T.E. Memorandum No. M.363 - A.R.C. 24,587

CONTENTS

TABLES

ILLUSTRATIONS

ILLUSTRATIONS (cont'd)

The log true stress/log natural strain relations for the mild steel and Rex 583 are compared in Figure 2(b).

4.0 Average tangential stress and measured strain

It was not possible to cover the complete plastic range of a rotor in a single test due to the difficulty of maintaining reasonable concentricity with the drive while plastic growth of up to 20 per cent took place in the bore. The rotors were therefore subjected to a number of repeated loadings, increasing with each test until burst took place. However, this feature made it possible to observe the plastic stress/strain behaviour of a rotor from measured distortion following each test.

As the speed of the model rotors increase from zero to the point of burst local high elastic stress enters the plastic range and redistribution of stress takes place. A small amount of plastic yielding in the rotor bore results in the tangential stress in Figure 1 rapidly approaching the average value. The average of the tangential stress is therefore a useful datum stress within the plastic range and the nominal value based on the original dimensions of the rotors and the speed may be calculated in the following manner:-

$$\text{Average tangential stress} = \frac{W \cdot \omega^2 \cdot r}{g \cdot A}$$

$$= 101.9 \left(\frac{RPM}{10^5}\right)^2 \text{ tons/sq in.}$$

where

W = half total weight of rotor

ω = angular velocity

r = radius of CG of half rotor

A = cross-sectional area through rotor

$g = 32.2 \text{ ft/s}^2$

The nominal average tangential stress at maximum speed for each rotor has been compared with the material ultimate tensile strength in a summary of results in Table IX.

Following the small amount of initial yielding the whole rotor rapidly becomes plastic as speed increases and the bore assumes a pronounced barrel shape. This is shown in Figure 3 in which the plastic deformation in the rotor, recorded in Tables IV, V and VI, has been plotted against the change in axial thickness. Substantial plastic deformation changes the stress level in the rotor and a correction to the average tangential stress related to the tangential strain in the bore is shown in Figure 4.

4.1 Yield point

Both mild steel and Rex 583 exhibit a yield point and this brings to light an important feature of the rotors. In Figures 5(a) and 5(b) the yield point in the rotor is higher than that in the test piece and would confirm the influence of the combined radial and tangential stresses.

4.2 Axial strain in bore

In order to study the influence of a wide hub on the conditions in the bore, the bore was polished and a strain grid lightly scribed on the surface. The axial strain measured at progressively increasing speeds within the material plastic range has been plotted in Figure 6.

The axial strain, ε_3, at the edge of the bore is negative and half the value of the tangential strain, ε_1. In the mid-bore region, however, considerable axial strain has occurred. This again is negative but equal in magnitude to the tangential strain as shown in Figure 7. The significance of the measured strain in the bore will be seen in the following analysis.

5.0 Plastic stress/strain analysis

The plastic strain in a rotor is the result of combined radial, tangential and axial loading. To obtain the stress distribution in a rotor it is therefore necessary to introduce theoretical equations relating plastic stress and strain under conditions of multiaxial loading. The equations for plasticity in the following analysis are due to Von Mises and Hencky[4].

In the first instance the distribution of strain in the rotor must be established and the data from a rotor in Rex 583 steel following a speed of 79,300 rev/min (Table VIII) has been selected for the analysis. These data produce only a limited number of points in Figure 8 but, by careful interpolation, it is possible to obtain the distribution of strain to an acceptable degree of accuracy. Points in the bore have been deduced from observations made in the previous Section 4.2. In addition, it has been assumed that no change in volume has occurred and the three principal strains may be related in the following manner:-

$$\varepsilon_1 + \varepsilon_2 + \varepsilon_3 = 0$$

The following equations for the significant stress and strain in a multiaxial stress system are based on distortion energy theory (Von Mises):-

$$\bar{\sigma} = \frac{\sqrt{2}}{2}\left[(\sigma_1 - \sigma_2)^2 + (\sigma_2 - \sigma_3)^2 + (\sigma_3 - \sigma_1)^2\right]^{\frac{1}{2}}$$

$$\bar{\varepsilon} = \frac{\sqrt{2}}{3}\left[(\varepsilon_1 - \varepsilon_2)^2 + (\varepsilon_2 - \varepsilon_3)^2 + (\varepsilon_3 - \varepsilon_1)^2\right]^{\frac{1}{2}}$$

where σ_1, σ_2 and σ_3 are the principal stresses and ε_1, ε_2 and ε_3 the resulting principal strains. The constants $\frac{\sqrt{2}}{2}$ and $\frac{\sqrt{2}}{3}$ are so chosen that $\bar{\sigma} = \sigma_1$ and $\bar{\varepsilon} = \varepsilon_1$ for simple uniaxial tension.

Stress and strain may be related by the Hencky deformation theory in the following equations:-

$$\varepsilon_1 = \frac{\bar{\varepsilon}}{\bar{\sigma}} \left[\sigma_1 - \frac{1}{2} \quad (\sigma_2 + \sigma_3)\right]$$

$$\varepsilon_2 = \frac{\bar{\varepsilon}}{\bar{\sigma}} \left[\sigma_2 - \frac{1}{2} \quad (\sigma_1 + \sigma_3)\right]$$

$$\varepsilon_3 = \frac{\bar{\varepsilon}}{\bar{\sigma}} \left[\sigma_3 - \frac{1}{2} \quad (\sigma_1 + \sigma_2)\right]$$

In Figure 9 the stress ratios have been obtained by introducing the strain plotted in Figure 8 into the Hencky equations.

In Figures 10(a) and 10(b) curves of maximum principal stress/strain have been plotted for various conditions of triaxial stress. These curves have been calculated from the simple tensile data of Figure 2(a) using the equations of Von Mises. Tangential strain from Figure 8 has then been superimposed using the stress ratio in Figure 9 and the distribution of tangential stress/strain in the rotor obtained. Finally in Figure 11 the distribution of stress has been plotted. The dotted line on this Figure is the corrected value of the average tangential stress (Section 4.0), which would appear to confirm the accuracy of the analysis. The low value of stress at the centre of the rotor is due to a compressive stress which is not accounted for in the calculation of the average tangential stress. This compressive stress which may be more clearly observed in Figure 12 is confirmed by a photo-elastic investigation on a similar shaped hub[3].

6.0 Tensile test data (biaxial)

Burst tests on simple discs[1] show that failure is the result of a biaxial tension produced by the combined radial and tangential stresses.

There is strong evidence in Figures 14, 15, 18, 19, 20 and 21 which suggests that failure originated from a point near the rim of the model rotors. (Note ductile behaviour at secondary failure point.) In addition, the foregoing analysis has shown that a maximum biaxial tension of 0.7 stress ratio occurs near the rim. A piece of the Rex 583 disc material was therefore tested in biaxial tension at the same stress ratio. This was achieved by loading the tube by means of internal hydraulic pressure and tension. The nominal results are shown in the following Table and tangential strain should be compared with R of A and elongation in Section 3.0:-

	Rex 583
Axial/tangential stress ratio	0.7
Nominal maximum tangential stress, tons/sq in.	66.7
Maximum tangential strain, %	2.6

In Figure 13 the results of the biaxial test are compared with the plastic stress/strain at the rim of the rotor. The tube exhibits the same low value of strain at burst as that measured on the rotor and it should be noted that values of strain for both rotor and tube are lower than that expected for theoretical instability.

7.0 Changes in rotor geometry

A number of changes in the initial geometry of the model rotor were made and the influence of each change on rotor burst strength is discussed in the following Sections.

The results are recorded in the summary of burst results in Table IX.

7.1 Axial keyway in bore

An axial keyway 0.025 in. radius and 0.025 in. deep, was machined in the bore of a model rotor Code 3/Rex 583/III, the cross-sectional area through the rotor being reduced locally by 1.5 per cent.

The burst test showed that a keyway of these proportions had no apparent influence on the strength of the rotor. Examination of the burst fragments Figure 20 suggests that the initial failure occurred near the rim, as in the other rotors, being followed by fracture through the keyway as the rotor opened outwards.

7.2 Increase in axial width

The axial width at the hub of rotor Code 3/Rex 583/IV was increased from 1.755 to 2.265, an increase of 29 per cent. The bore was also increased.

The following value of the average tangential stress was calculated for the wide hub model:-

$$\text{Average tangential stress} = 94.6\left(\frac{\text{RPM}}{10^5}\right)^2 \text{ tons/sq in.}$$

The burst test showed a reduction in both rotor strength and ductility. The axial strain at Points C and D recorded in Table IX show that the slope of the sides on this model at burst was much greater than on the initial geometry and indicates that the bore had taken up a more pronounced barrel shape.

7.3 Reduction in rim loading

The rim loading was reduced by 6.5 per cent on rotor Code 4/Rex 583/IV by reducing the overall diameter of the model from 5.54 in. to 5.28 in. This resulted in the following reduced value for the average tangential stress:-

$$\text{Average tangential stress} = 86.0\left(\frac{\text{RPM}}{10^5}\right)^2 \text{ tons/sq in.}$$

In this test the rotor exhibited substantial ductility at burst, the reduction in axial dimensions C and D recorded in Table IX being approximately twice that for the standard model rotor.

A reduction in rim loading would reduce the radial stress and hence the maximum stress ratio and an increase in material ductility would be expected.

8.0 Conclusions

A number of model steam turbine rotors in mild steel, cast iron and 3 per cent Cr.Mo.V. steel (Rex 583) have been spun to burst and the following conclusions drawn from the results:-

(i) A detailed plastic stress analysis shows that a wide hub introduces a substantial compressive stress in the mid-bore region and this has been confirmed by photo-elastic analysis on similar rotor hubs. An improvement in material ductility would be expected due to the axial compression but this has been revealed in the models by local plastic deformation in the mid-bore region at low rotational speeds, i.e., as low as 46,000 rev/min.

(ii) Increases in rotor hub width reduce the tangential stress at the bore but do not alleviate the biaxial tension at the rim. Biaxial tension considerably reduces the ductility of a material and, in these rotors, biaxial tension at the highest value of stress ratio has undoubtedly been the cause of failure and has had a stronger influence than a keyway in the bore. Similar, low values of ductility have been exhibited by tubes of disc material subjected to the same maximum ratio of biaxial tension.

(iii) It would appear that rotor strength might be increased by reducing the degree of biaxial tension at the rim. This has been demonstrated on one model which exhibited a substantial increase in ductility when the rim loading was reduced. However, some reduction in biaxial tension could be achieved by designing the rotor with convex rather than concave sides. An additional advantage of this change in geometry would be a reduced tendency to early yielding in the mid-bore region.

NOTATION

σ'	nominal stress	
ε'	nominal strain	
σ	true stress $= \sigma' (1 + \varepsilon')$	
ε	natural strain $= \log_e (1 + \varepsilon')$	
K	strength coefficient	in the relation $\sigma = K\varepsilon^n$
n	strain hardening exponent	
σ_1 and ε_1	true tangential stress and strain (maximum principal)	
σ_2 and ε_2	true radial stress and strain	
σ_3 and ε_3	true axial stress and strain	
$\bar{\sigma}$ and $\bar{\varepsilon}$	significant or uniaxial equivalent stress and strain	
ω	angular velocity	
W	half total weight of rotor	In relation to average tangential stress calculation
r	radius of CG of half rotor	
A	cross-sectional area through rotor	
g	constant $= 32.2$ ft/s^2	
r	radius of CG of half rotor or	
	mean radius of tube wall	In relation to tubes with internal hydraulic pressure and tension
P	Hydraulic pressure	
t	tube wall thickness	

REFERENCES

No.	Author(s)	Title, etc.
1	M. E. Waldren D. E. Ward	Room temperature instability and fraction in rotating discs and correlation with bi-axial tensile test data. A.R.C. C.P. 660 January 1963
2	F. Dollin	Some design problems arising in the development of very large high-speed turbines. I.Mech.E. November 1962
3	H. Fessler E. I. May E. A. Roberts	Centrifugal stresses at the bores of wheels. The Engineer, Technical Contributors Section. January 1961
4	G. E. Dieter, Jnr.	Mechanical Metallurgy, McGraw Hill, 1961

TABLE I(a)

Tensile test data - material Code 1/MS/P1

	Code	Nominal stress - tons/sq in.					Nominal strain			True ultimate		
							Fracture		Ultimate	Stress	Strain	
	Code	LP	0.1% proof	Ult	0.1% proof / Nom ult	Frac	R of A %	Elong %	1 + elong = $\left(\frac{d_o}{d}\right)^2$	ult × $\left(\frac{d_o}{d}\right)^2$	$\log_e \left(\frac{d_o}{d}\right)^2$	
Radial	1/MS/P1/A1a	11.36	16.24	34.4	0.473	27.2	60.0	33.0	1.32	45.4	0.278	
Radial	1/MS/P1/A1b	12.28	16.16	33.2	0.487	29.6	37.8	19.0	1.159	38.5	0.1476	
Tangential	1/MS/P1/A2a	11.2	16.6	34.0	0.488	26.4	55.0	33.2	1.229	41.8	0.207	
Tangential	1/MS/P1/A2b	8.6	16.4	33.8	0.486	26.6	56.3	33.4	1.31	44.3	0.27	
Tangential	1/MS/P1/A4a	7.2	13.0	33.6	0.387	27.6	55.3	34.0	1.276	42.9	0.244	Within disc geometry
Tangential	1/MS/P1/A4b	4.8	13.2	33.4	0.396	26.4	52.6	32.0	1.292	43.2	0.256	Within disc geometry
Bore axial	1/MS/P1/A5a	12.8	15.8	33.2	0.476	25.2	63.2	38.0	1.336	44.4	0.2896	
Bore axial	1/MS/P1/A5b	11.2	14.88	34.0	0.438	26.0	63.2	35.0	1.276	43.4	0.2438	

TABLE I(b)

Tensile test data - material Code 1/MS/P1/A2 and A4

1/MS/P1/A2(b)	Stress - tons/sq in.		Plastic strain	
	Nominal σ'	True $\sigma = \sigma'(1+\varepsilon')$	Nominal $1+\varepsilon'$	Natural $\varepsilon = \log_e 1+\varepsilon'$
LP	8.6	8.6	0	0
0.1% proof	16.4	16.4	1.001	0.001
	18.0	18.1	1.008	0.008
	19.2	19.5	1.016	0.016
	21.2	21.9	1.032	0.032
	24.0	25.5	1.063	0.061
	26.3	28.8	1.095	0.093
	28.3	31.9	1.127	0.119
	29.9	34.6	1.158	0.147
	31.2	37.1	1.190	0.174
	32.0	39.0	1.222	0.201
	32.7	41.0	1.254	0.226
	33.2	42.7	1.285	0.251
	33.6	44.3	1.316	0.275
Ultimate	33.8		(1.35)	(0.30)
Fracture	26.6	61.0	2.29	0.829

1/MS/P1/A4(b)	Stress - tons/sq in.		Plastic strain	
	Nominal σ'	True $\sigma = \sigma'(1+\varepsilon')$	Nominal $1+\varepsilon'$	Natural $\varepsilon = \log_e 1+\varepsilon'$
LP	4.8	4.8	0	0
0.1% proof	13.2	13.2	1.001	0.001
	20.2	20.6	1.016	0.016
	22.6	23.2	1.024	0.024
	24.8	25.6	1.032	0.032
	26.2	27.2	1.040	0.039
	27.6	28.9	1.048	0.047
	28.6	30.2	1.055	0.054
	29.4	31.3	1.063	0.062
Ultimate	33.4		(1.29)	(0.255)
Fracture	26.4	70.5	2.67	0.982

TABLE II

Tensile test data - material Code 1/C1/P1

	Code	Nominal stress - tons/sq in.					Nominal strain			True ultimate		
							Fracture		Ultimate	Stress	Strain	
		LP	0.1% proof	Ult	$\frac{0.1\% \text{ proof}}{\text{Nom ult}}$	Frac	R of A %	Elong* %	$1 + \text{elong} = \left(\frac{d_o}{d}\right)^2$	$\text{ult} \times \left(\frac{d_o}{d}\right)^2$	$\log_e \left(\frac{d_o}{d}\right)^2$	
Radial	1/C1/P1/A1a	6.8	11.3	14.8	0.754			2.0				
Radial	1/C1/P1/A1b	5.0	11.6	14.68	0.79			2.0				
Tangential	1/C1/P1/A2a	6.0	12.8	15.24	0.839			2.0				
Tangential	1/C1/P1/A2b	4.2	9.76	10.6	0.921			1.0				
Tangential	1/C1/P1/A4a	5.2	11.6	17.9	0.649	AS FOR ULT		2.5				Within disc geometry
Tangential	1/C1/P1/A4b	5.2	11.6	18.0	0.644			4.5				
Bore axial	1/C1/P1/A5a	4.2	8.2	13.3	0.616			2.5				
Bore axial	1/C1/P1/A5b	5.2	9.4	14.2	0.662			3.0				
Bore axial	1/C1/P1/A5c	5.2	10.7	13.2	0.812			3.0				
Bore axial	1/C1/P1/A5d	5.3	9.3	14.0	0.664			3.0				

Note
All specimens and discs from single casting 6 in. diameter 15 in. long cast vertically in sand. No subsequent heat treatment.

*These readings appear high and may be due to difficulty in measuring elongation on $\frac{1}{40}$ sq in. specimens. Experience suggests values about 0.5 per cent (see Figure 2(a)).

TABLE III(a)

Tensile test data - material Code 3/Rex 583

	Code	Nominal stress - tons/sq in. LP	0.1% proof	Ult	$\frac{0.1\% \text{ proof}}{\text{Nom ult}}$	Frac	Nominal strain: Fracture R of A %	Fracture Elong %	Ultimate 1 + elong $= \left(\frac{d_o}{d}\right)^2$	True ultimate: Stress ult $\times \left(\frac{d_o}{d}\right)^2$	Strain $\log_e \left(\frac{d_o}{d}\right)^2$
Tangential	3/R583/A4a	22.8	44.9	66.8	0.673	50.8	48.9	20	1.086	72.6	0.0827
	3/R583/A4b	25.2	45.8	67.2	0.682	52.4	44.7	18	1.099	73.9	0.0948
	3/R583/A4c	20.8	44.4	67.8	0.655	52.8	48.7	20	1.078	73.1	0.0753
	3/R583/A4d	25.6	47.2	67.5	0.698	52.4	47.4	20	1.084	73.3	0.0808
Axial	3/R583/A5a	26.4	44.0	68.0	0.647	53.6	45.2	18	1.096	74.6	0.0919
	3/R583/A5b*	26.4	51.4	67.2	0.764	50.2	53.0	19	1.090	73.4	0.0862
	3/R583/A5c‡	-	-	68.8	-	53.2	48.9	18	1.078	74.1	0.0753

* Interrupted test to examine influence of pre-straining

‡ High rate of loading approximately 4 tons/sq in./s

TABLE III(b)

Tensile test data - material Code 3/Rex 583/A4(b)

	Stress - tons/sq in.		Plastic strain	
	Nominal σ'	True $\sigma = \sigma'(1 + \varepsilon')$	Nominal $1 + \varepsilon'$	Natural $\varepsilon = \log_e 1 + \varepsilon'$
LP	25.2	25.2	0	0
0.1% proof	45.8	45.8	1.001	0.001
	53.0	53.2	1.005	0.005
	57.6	58.5	1.011	0.011
	60.4	61.5	1.019	0.019
	63.0	64.7	1.027	0.026
	64.4	66.6	1.035	0.034
Ultimate	67.2		(1.10)	(0.095)
Fracture	52.4	95.5	1.82	0.600

TABLE IV

Stress/strain data - model disc Code 1/MS/P1/I

Speed rev/min	Zero	48,000	50,100	52,500	55,000	55,800		55,200
Nom av tan stress } t.s.i.	-	21.5	25.5	29.0	31.5	31.9		31.0
Corr av tan stress } t.s.i.	-	22.0	26.8	31.4	35.8	36.7		39.7
$A/A_0 = (1 + \varepsilon_1')$	1.000		1.053 1.051	1.088 1.082	1.143 1.132	1.155 1.147		
$B_1/B_{1.o} = (1 + \varepsilon_1')$	1.000	1.023	1.032	1.053 1.045	1.110 1.085	1.117 1.093		
$B_2/B_{2.o} = (1 + \varepsilon_1')$	1.000	1.023	1.035	1.062 1.048	1.056 1.072	1.096 1.088		
$C_o/C = (1 + \varepsilon_3')$	1.000	1.016	1.042	1.059	1.082	1.103 1.092		1.169
$D_o/D = (1 + \varepsilon_3')$	1.000	1.015	1.018	1.028	1.048 1.028	1.051 1.045		1.071
$E/E_o = (1 + \varepsilon_1')$	1.000	1.009	1.015	1.022	1.033	1.040 1.036		
$F_1/F_{1.o} = (1 + \varepsilon_1')$	1.000	1.007	1.014	1.021	1.037 1.032	1.041 1.037		
$F_2/F_{2.o} = (1 + \varepsilon_1')$	1.000	1.007	1.014	1.030	1.047 1.037	1.048 1.040		

TABLE V

Stress/strain data - model disc Code 1/MS/P1/II

Speed rev/min	Zero	44,000	51,500	52,000	52,800	52,800	51,600	
Nom av tan stress } t.s.i.	-	20.0	27.5	28.1	28.9	28.9		
Corr av tan stress } t.s.i.	-	20.5	30.2	32.6	34.0	35.8		
$A/A_0 = (1 + \varepsilon_1')$	1.000		1.098 1.079	1.160 1.142	1.178 1.169	1.238 1.214		
$B_1/B_{1.0} = (1 + \varepsilon_1')$	1.000	1.017	1.067 1.052	1.103 1.085	1.124 1.108	1.158 1.126		
$B_2/B_{2.0} = (1 + \varepsilon_1')$	1.000	1.022	1.071 1.052	1.126 1.092	1.133 1.108	1.195 1.148		
$C_0/C = (1 + \varepsilon_3')$	1.000	1.019 1.017	1.058 1.050	1.087 1.079	1.102 1.086	1.140 1.108	1.120	
$D_0/D = (1 + \varepsilon_3')$	1.000	1.012 1.006	1.038 1.034	1.060 1.034	1.066 1.052	1.088 1.002	1.070	
$E/E_0 = (1 + \varepsilon_1')$	1.000	1.008	1.023 1.021	1.042 1.036	1.047 1.041	1.060 1.052		
$F_1/F_{1.0} = (1 + \varepsilon_1')$	1.000	1.000	1.025 1.013	1.041 1.027	1.050 1.030	1.064 1.038		
$F_2/F_{2.0} = (1 + \varepsilon_1')$	1.000	1.012 1.007	1.031 1.021	1.056 1.032	1.054 1.036	1.085 1.047		

TABLE VI

Stress/strain data - model disc Code 1/MS/P1/III

Speed rev/min	Zero	42,200	43,200	44,300	45,300	46,400	47,500	49,600	51,100	54,300	55,900	57,200
Nom av tan stress } t.s.i.	-	18.1	19.0	20.0	20.9	21.9	23.0	25.1	26.3	30.0	31.7	33.3
Corr av tan stress } t.s.i.	-	18.1	19.25	20.3	21.4	22.6	23.7	26.2	27.8	33.0	36.5	40.3
$A/A_o = (1 + \varepsilon_1')$	1.000	1.001	1.013	1.018	1.022	1.031	1.031	1.045 1.042	1.059 1.057	1.104 1.100	1.156 1.143	1.224 1.196
$B_1/B_{1.o} = (1 + \varepsilon_1')$	1.000	1.000	1.007	1.011	1.014	1.018	1.019	1.027	1.036 1.031	1.060 1.052	1.095 1.083	1.125 1.100
$B_2/B_{2.o} = (1 + \varepsilon_1')$	1.000	1.000	1.008	1.012	1.015	1.017	1.019	1.028 1.026	1.037 1.035	1.076 1.068	1.121 1.096	1.208 1.148
$C_o/C = (1 + \varepsilon_3')$	1.000	1.001	1.008	1.010	1.012	1.014	1.015	1.024 1.022	1.032 1.029	1.056 1.050	1.083 1.079	1.104 1.098
$D_o/D = (1 + \varepsilon_3')$	1.000	1.000	1.004	1.006	1.007	1.008	1.009	1.013 1.011	1.018 1.016	1.032 1.026	1.050 1.043	1.073 1.050
$E/E_o = (1 + \varepsilon_1')$	1.000	1.000	1.002	1.004	1.005	1.006	1.006	1.012	1.016	1.025	1.039 1.034	1.052 1.046
$F_1/F_{1.o} = (1 + \varepsilon_1')$	1.000	1.000	1.003	1.004	1.005	1.007	1.007	1.012	1.014	1.023	1.042 1.037	1.052 1.038
$F_2/F_{2.o} = (1 + \varepsilon_1')$	1.000	1.000	1.000	1.003	1.005	1.006	1.006	1.011	1.014	1.027	1.047 1.038	1.087 1.053

Not burst (damaged)

TABLE VII

Axial strain in bore - model disc Code 1/MS/P1/III

Speed rev/min		46,400	47,500	49,600	51,100	54,300	55,900	57,200
Nom av tan stress (t.s.i.)		21.9	23.0	25.1	26.3	30.0	31.7	33.3
Corr av tan stress (t.s.i.)		22.6	23.7	26.2	27.8	33.0	36.5	40.3
Bore Edge - B1	1	0.008	0.033	0.041	0.155	0.016	0.073	-
	2	-	0.008	0.016	0.057	0.048	0.040	0.097
	3	0.032	0.024	0.040	0.048	0.057	0.073	0.105
	4	-	0.024	0.024	0.032	0.065	0.089	0.145
	5	0.032	0.032	0.032	0.048	0.065	0.089	0.129
	6	-	-	0.008	0.024	0.065	0.090	0.163
	7	0.008	0.017	0.017	0.041	0.041	0.083	0.123
Bore Mid.	8	-	0.040	0.040	0.048	0.112	0.119	0.191
	9	0.049	0.033	0.049	0.049	0.041	0.115	0.098
	10	0.108	0.075	0.085	0.081	0.129	0.136	0.218
	11	-	0.008	0.024	0.024	0.065	0.090	0.122
	12	0.040	0.040	0.040	0.040	0.095	0.095	0.167
	13	0.042	-	0.008	0.025	-	0.108	0.058
	14	-	0.008	0.018	0.031	0.217	0.062	-
Bore Edge - B2	15	0.070	0.061	0.052	0.061	-	0.061	-

Note: Axial strain $\varepsilon_s = 1 - \frac{t}{t_o}$ on 0.1 in. gauge lengths through bore

TABLE VIII

Stress/strain data - model disc Code 3/Rex 583/II

Speed rev/min	Zero	67,000	68,600	71,800	73,400	75,000	76,600	78,200	79,300	80,400
Nom av tan stress } t.s.i.	Zero	45.5	48.0	52.5	54.8	57.3	59.7	62.0	64.0	65.8
Corr av tan stress } t.s.i.	Zero	45.5	48.0	52.5	54.8	57.6	60.8	64.1	66.4	72
$A/A_c = (1 + \varepsilon_1')$	1.00	1.00	1.0023	1.00245	1.00245	1.0049	1.007	1.033	1.038	(1.095)
$B_1/B_{1.0} = (1 + \varepsilon_1')$	1.00	1.00	1.0007	1.00105	-	1.0012	1.0063	1.022 1.0175	1.030 1.022	-
$B_2/B_{2.0} = (1 + \varepsilon_1')$	1.00	1.00	1.00175	1.00209	1.0007	1.00209	1.0077	1.0174 1.01465	1.0216 1.0195	-
$C_0/C = (1 + \varepsilon_3')$	1.00	1.00	1.00114	1.0014	1.0017	1.0023	1.0051	1.015	1.020	1.050
$D_0/D = (1 + \varepsilon_3')$	1.00	1.00	-	-	1.0002	1.0006	1.0026	1.008	1.010	1.033
$E/E_0 = (1 + \varepsilon_1')$	1.00	1.00	1.00	1.00	1.00018	1.00072	1.0023	1.0065	1.008	-
$F_1/F_{1.0} = (1 + \varepsilon_1')$	1.00	1.00	1.00	1.00	1.0004	1.00077	1.00192	1.0082	1.0115	-
$F_2/F_{2.0} = (1 + \varepsilon_1')$	1.00	1.00	1.00	1.00	1.0004	1.00116	1.00193	1.00695	1.0093	-

TABLE IX

Summary of model rotor burst results

Rotor code	Maximum speed rev/min	Burst speed rev/min	Nom av tan stress at max. speed tons/sq in.	Material ultimate tensile strength tons/sq in.	Axial strain at burst C_o/C	Axial strain at burst D_o/D	Remarks
1/MS/P1/I	55,800	55,200	31.9		1.169	1.071	Speed measurement in doubt
1/MS/P1/II	52,800	51,600	28.9	33.5	1.120	1.070	
1/MS/P1/III	57,200	Not burst	33.3		(1.102)	(1.061)	
1/C1/P1/I	41,400		17.45				
1/C1/P1/II	41,100		17.20	18.0	Less than 0.1%		
1/C1/P1/III	40,100	38,800	16.40				
3/Rex 583/I	80,800		66.5		1.063	1.030	
3/Rex 583/II	80,400	78,800	65.8		1.050	1.033	
3/Rex 583/III	81,060		67.0	67.2	1.076	1.037	Axial keyway in bore .025 in. rad. x .025 in. deep
3/Rex 583/IV	81,180		63.0		1.054	1.020	Axial width increased 1.755 in. to 2.265 in.
4/Rex 583/IV	87,000	86,750	65.2		1.128	1.055	Rim loading reduced 5.54 in. to 5.28 in. o.d.

FIG. 1(a)

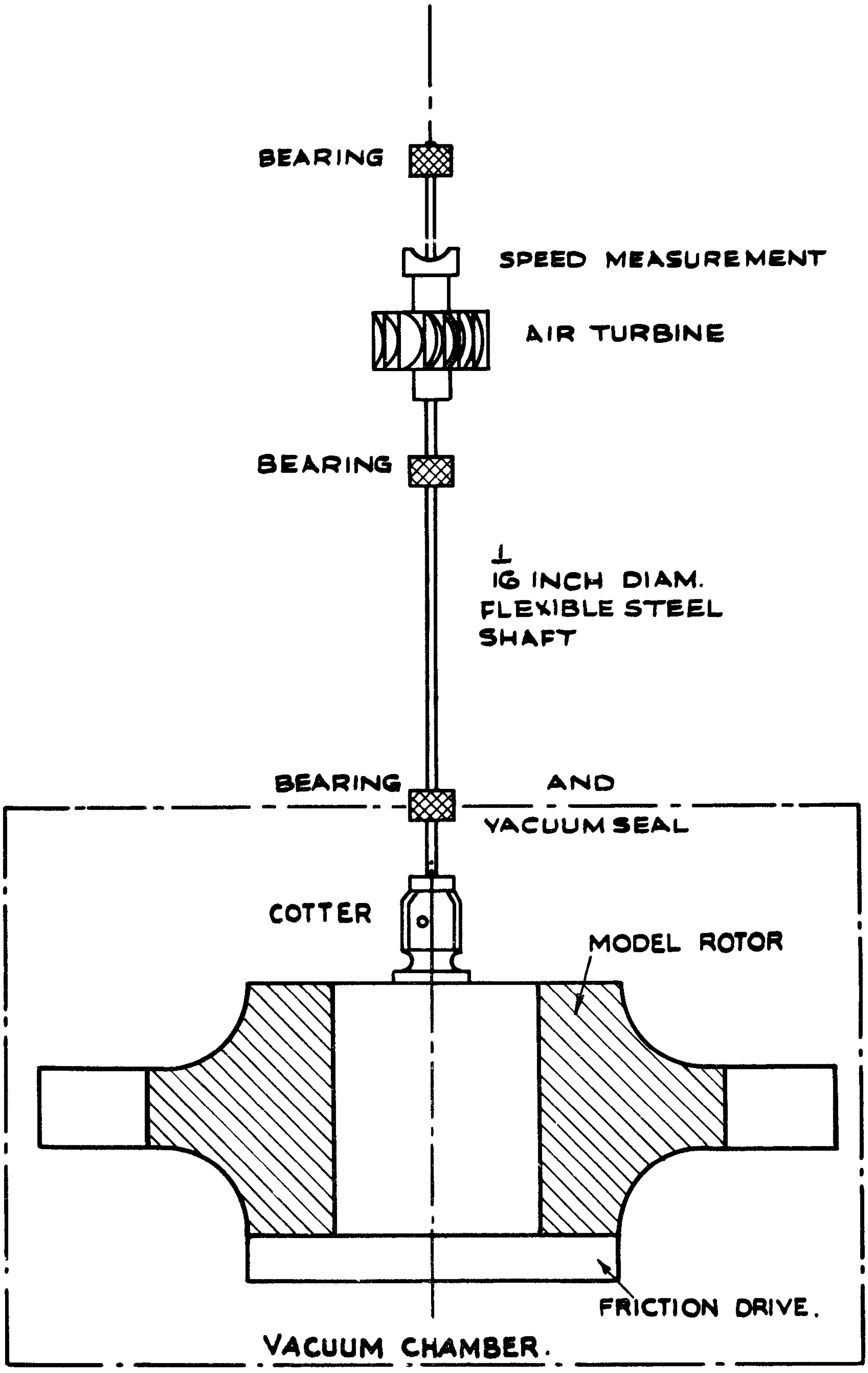

DIAGRAM OF ROTOR SPINNING RIG
(FULL SCALE)

FIG. 1(b)

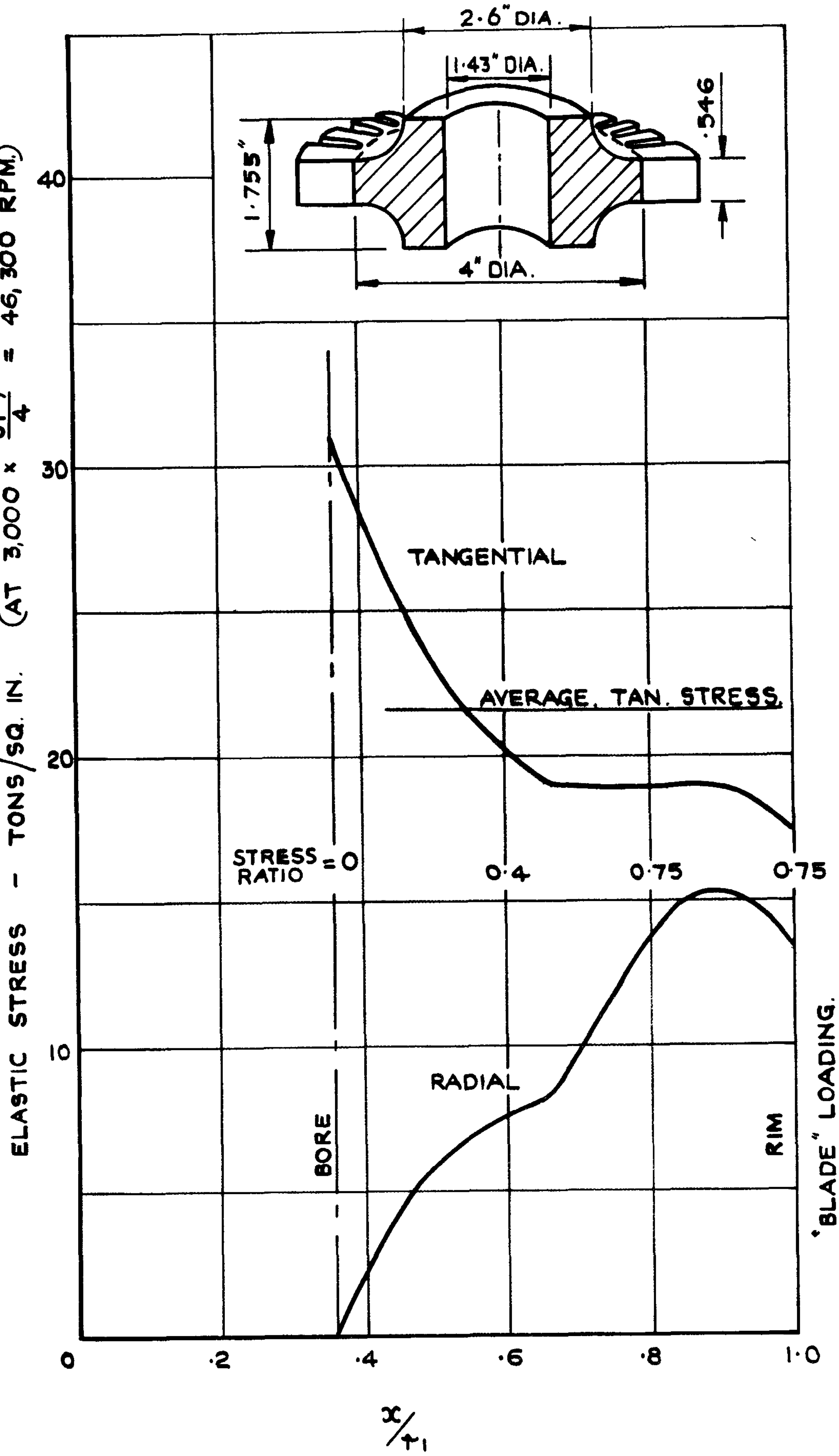

ELASTIC STRESS DISTRIBUTION IN MODEL ROTOR AT 46,300 RPM.

FIG. 2(a)

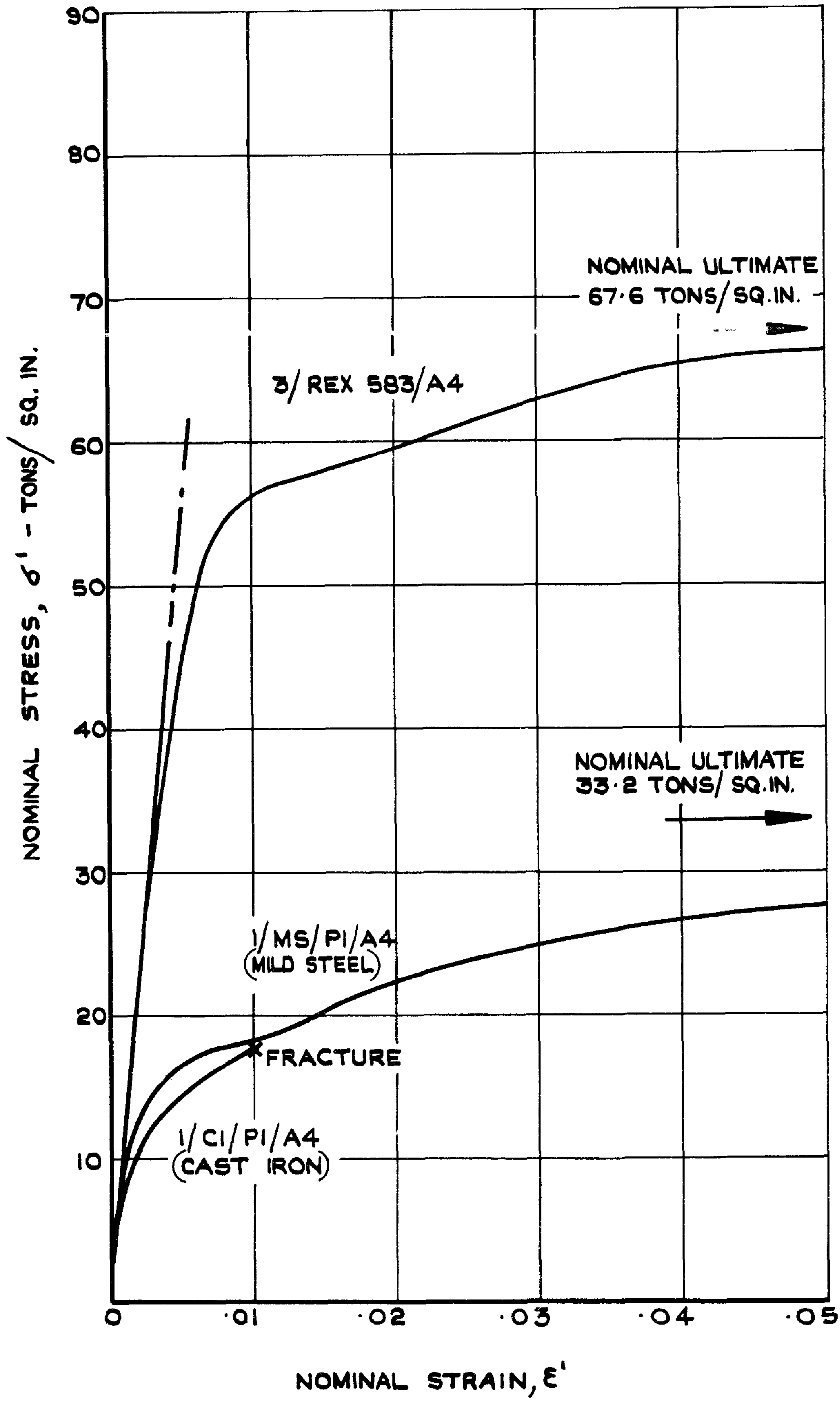

COMPARISON BETWEEN STRESS/STRAIN DATA FOR MILD STEEL, REX 583 & CAST IRON.

FIG. 2(b)

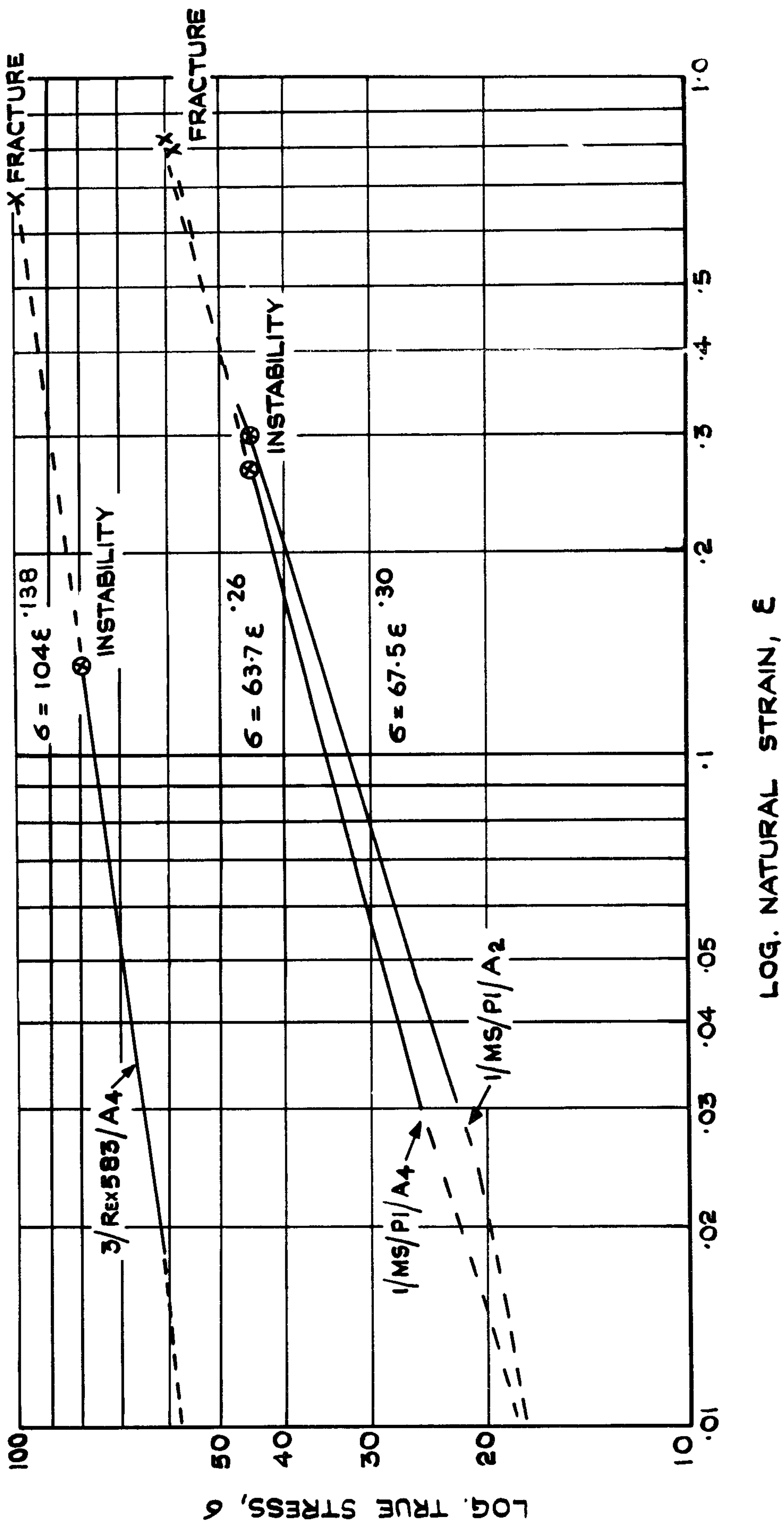

LOG TRUE STRESS/LOG NATURAL STRAIN DATA.

FIG. 3

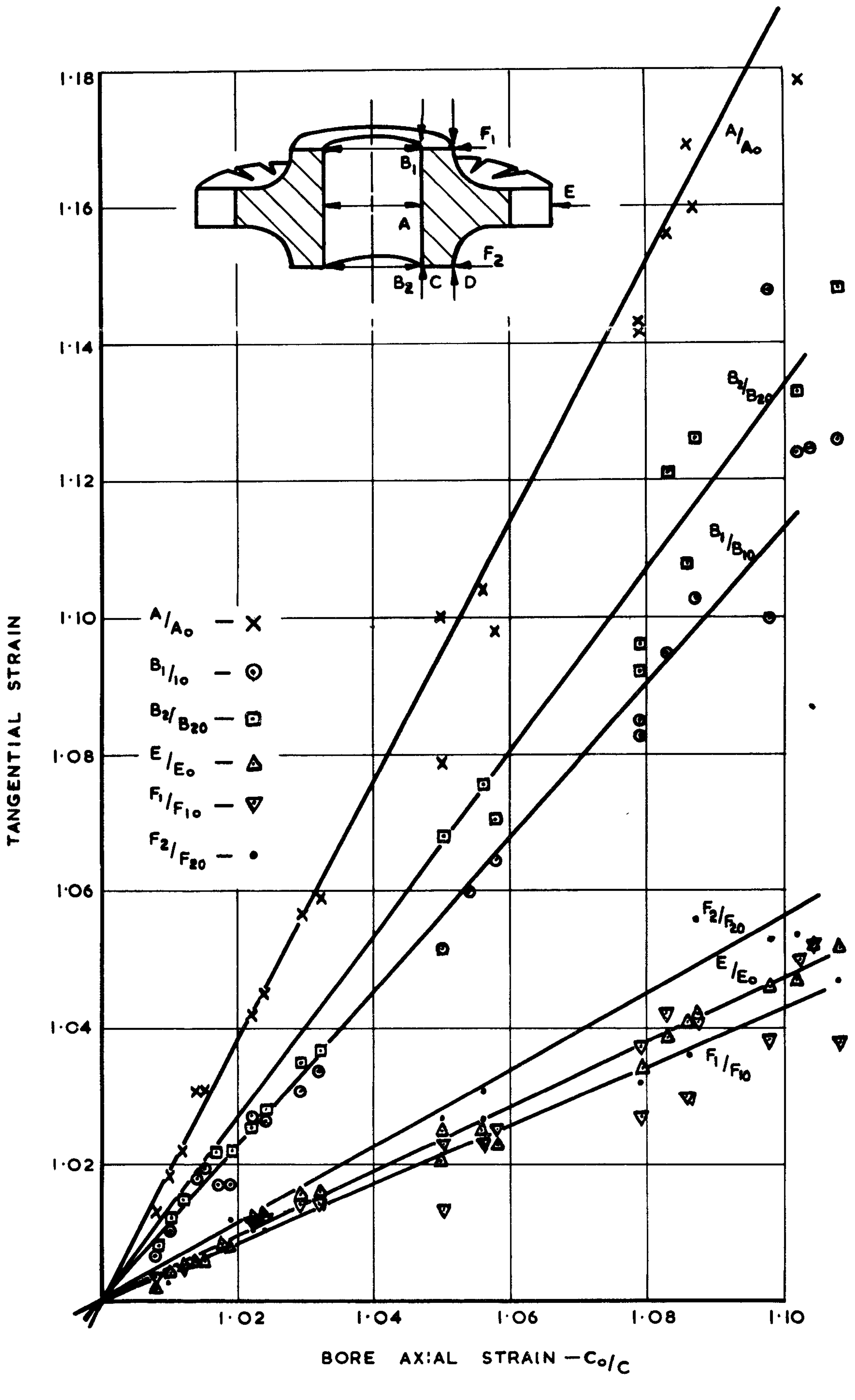

ROTOR TANGENTIAL STRAINS RELATED TO BORE AXIAL STRAIN.

FIG. 4

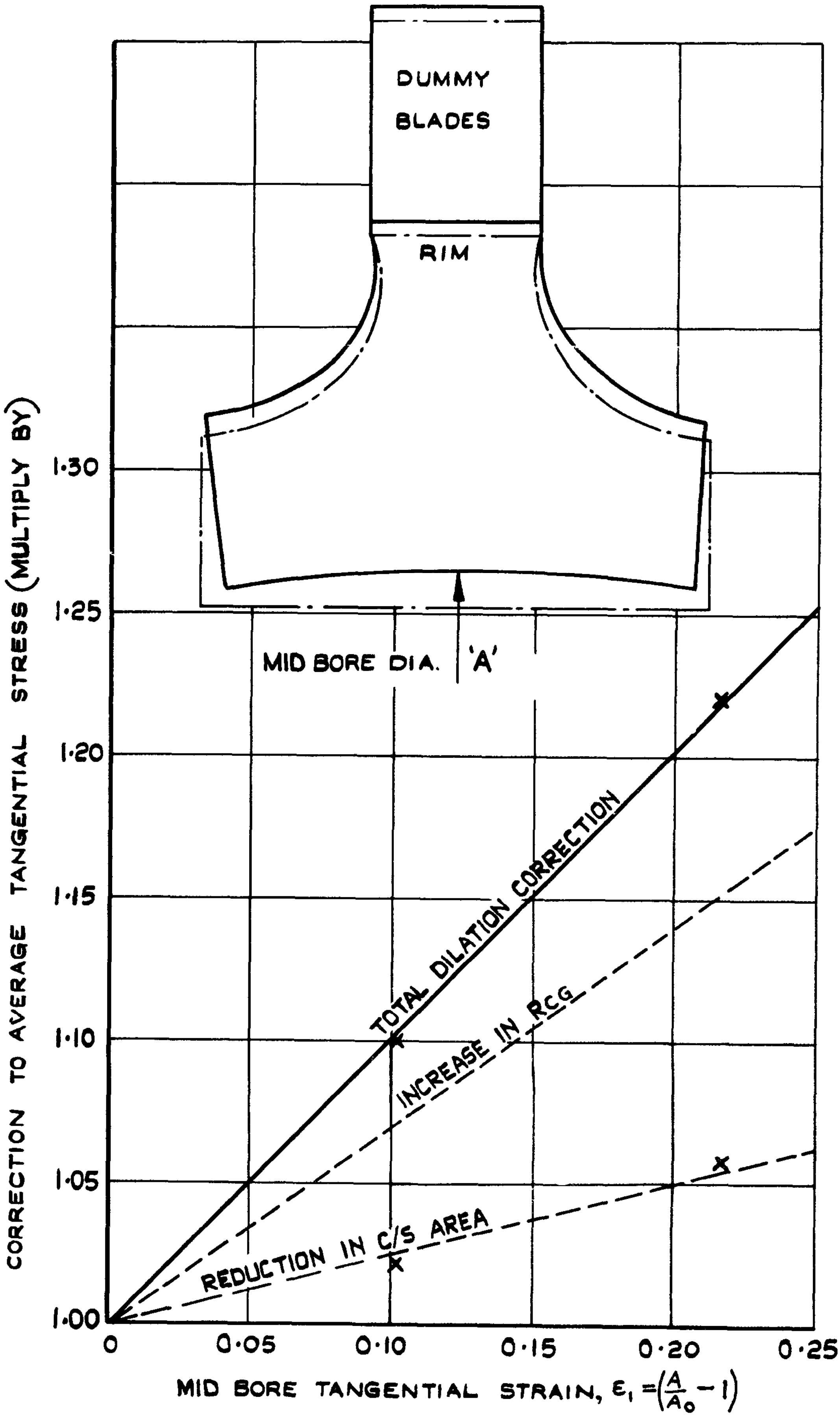

DILATION CORRECTION TO ROTOR AVERAGE TANGENTIAL STRESS

FIG. 5(a)

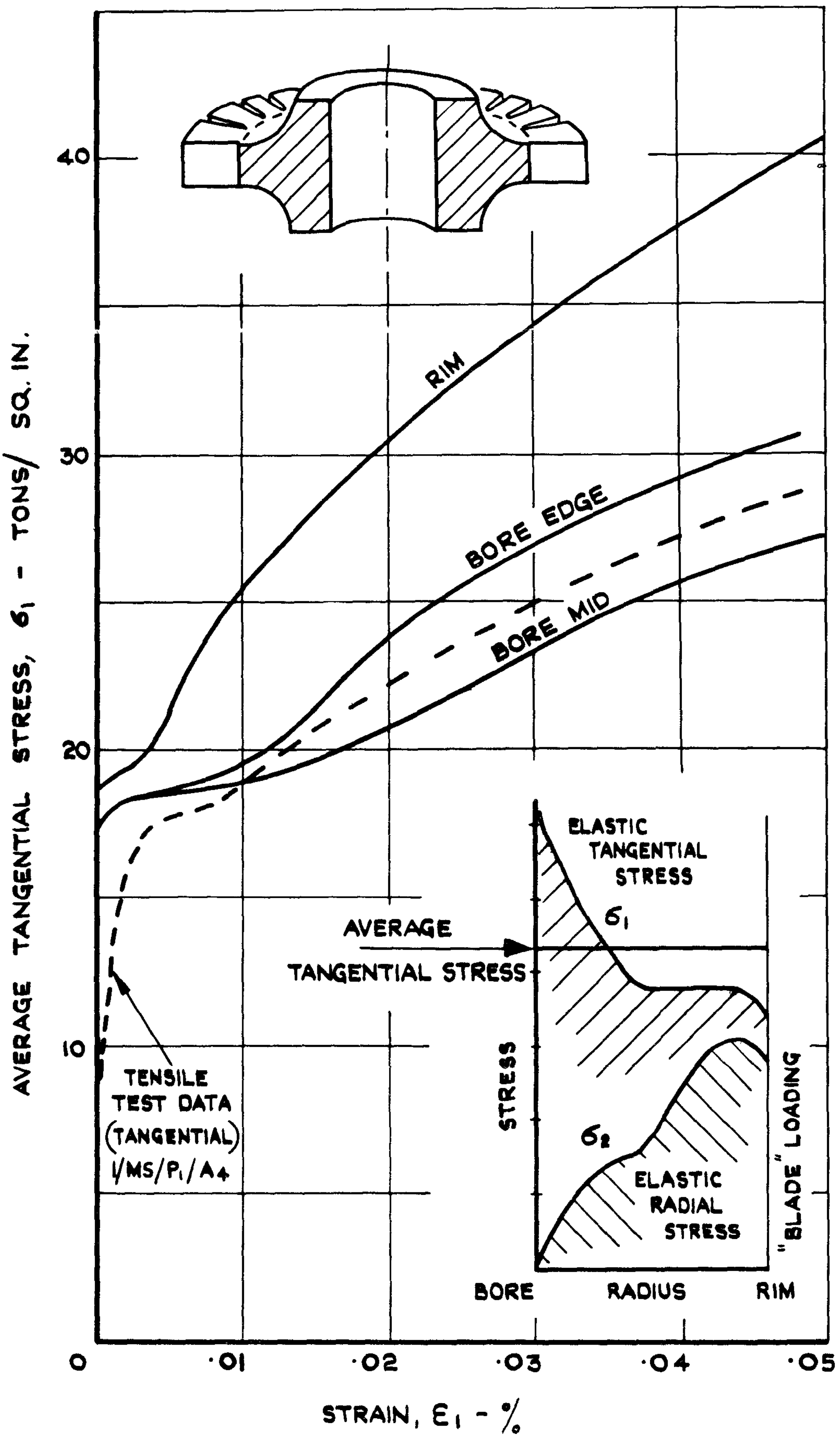

YIELD POINT IN MODEL ROTOR & TEST PIECE

MILD STEEL (UTS 33·5 TONS/ SQ. IN.)

FIG. 5(b)

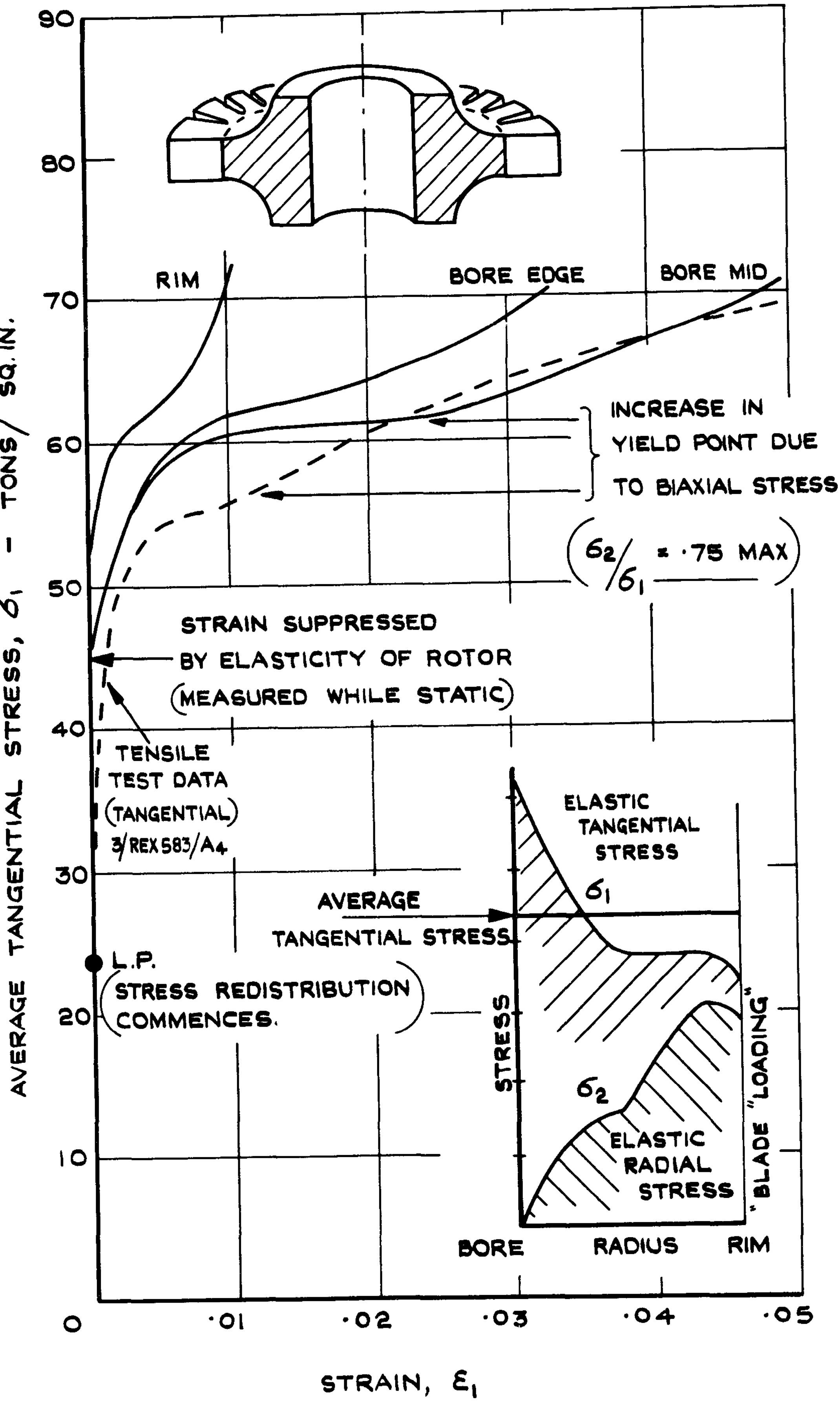

YIELD POINT IN MODEL ROTOR & TEST PIECE
REX 583 (UTS 67 TONS/SQ. IN.)

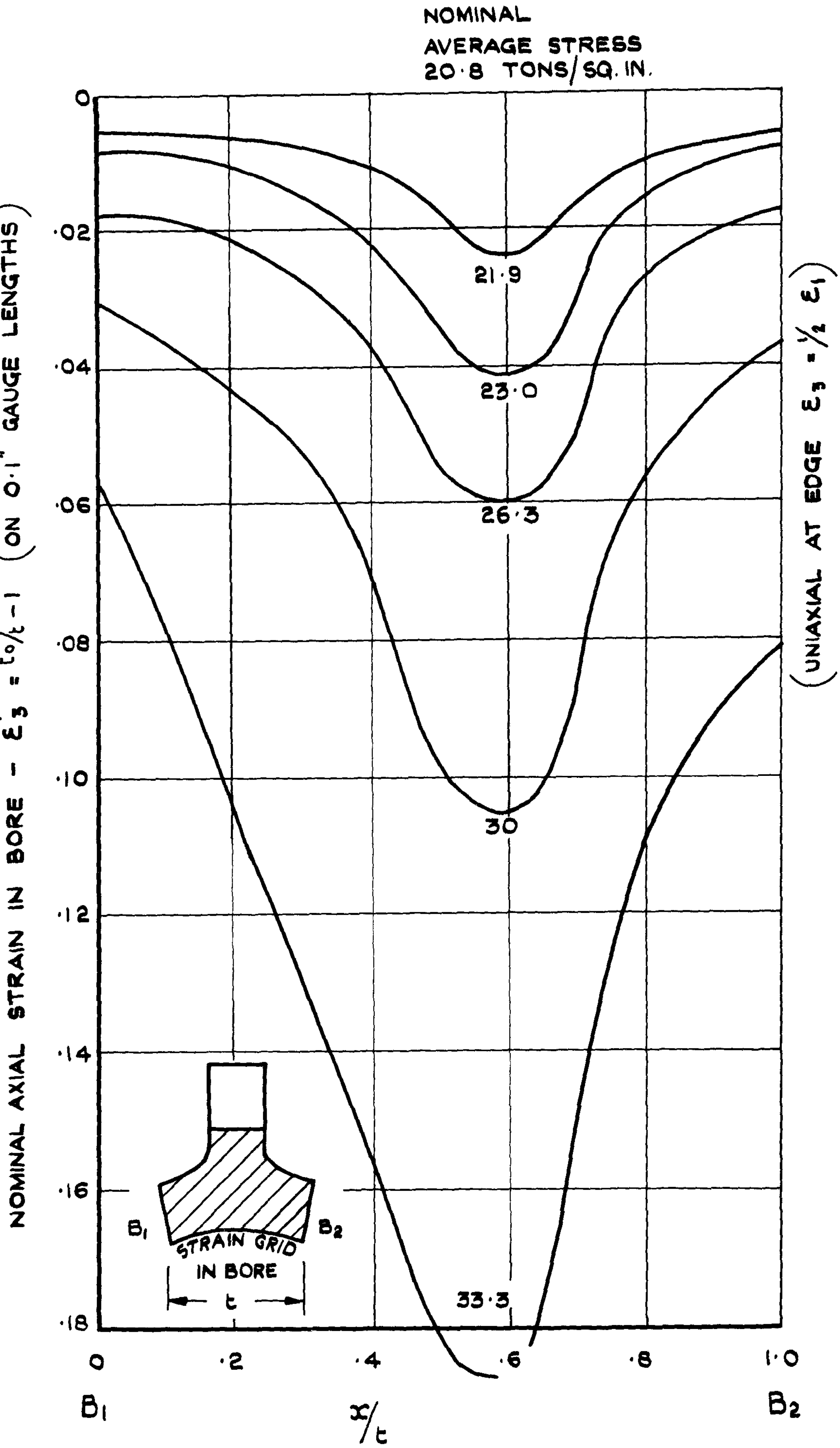

REDUCTION IN AXIAL WIDTH THROUGH BORE OF MODEL ROTOR - CODE I/MS/PI/III.

FIG. 7

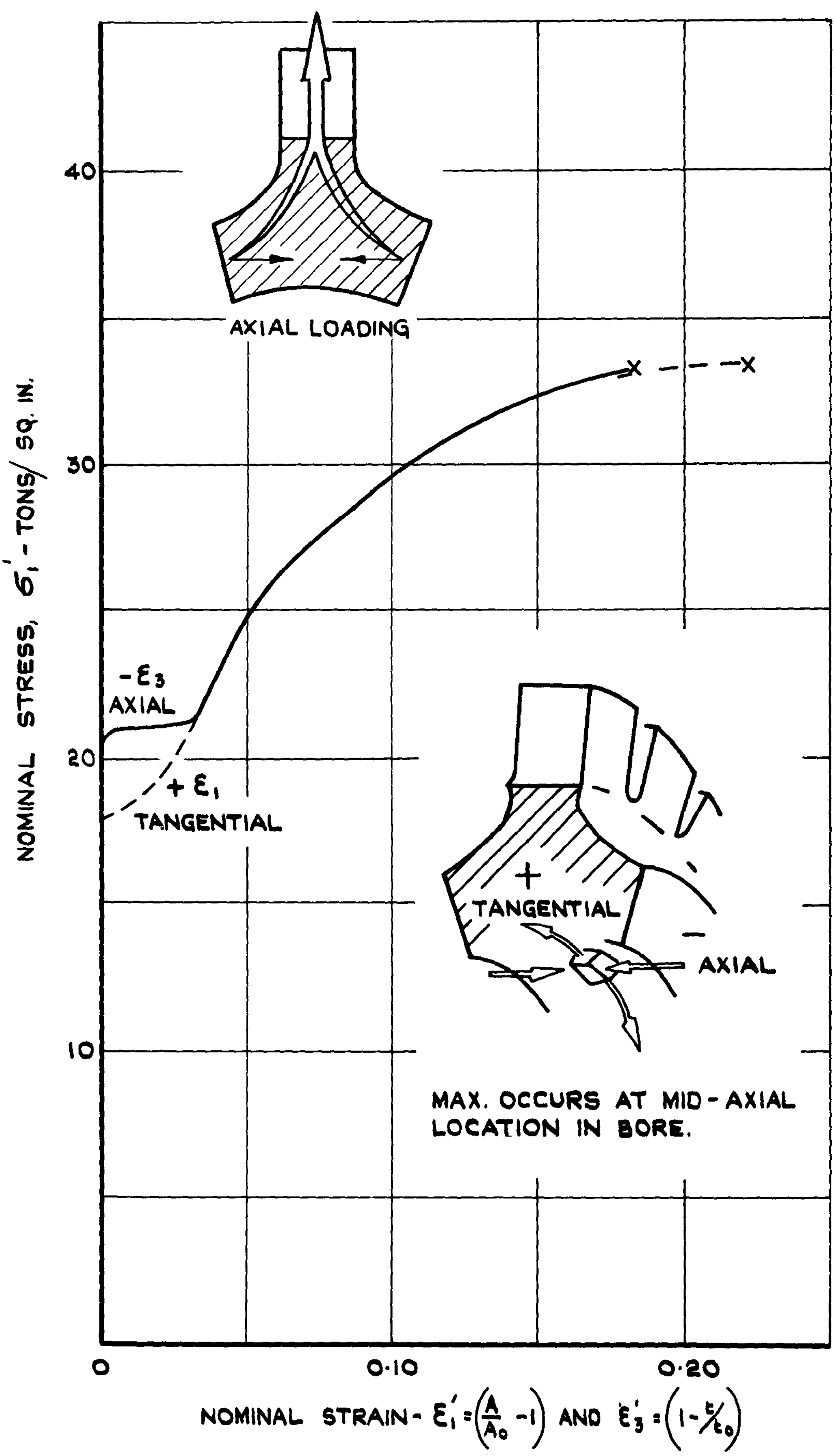

MAXIMUM TANGENTIAL & AXIAL STRAIN IN BORE OF MODEL ROTOR - CODE I/MS/PI/III.

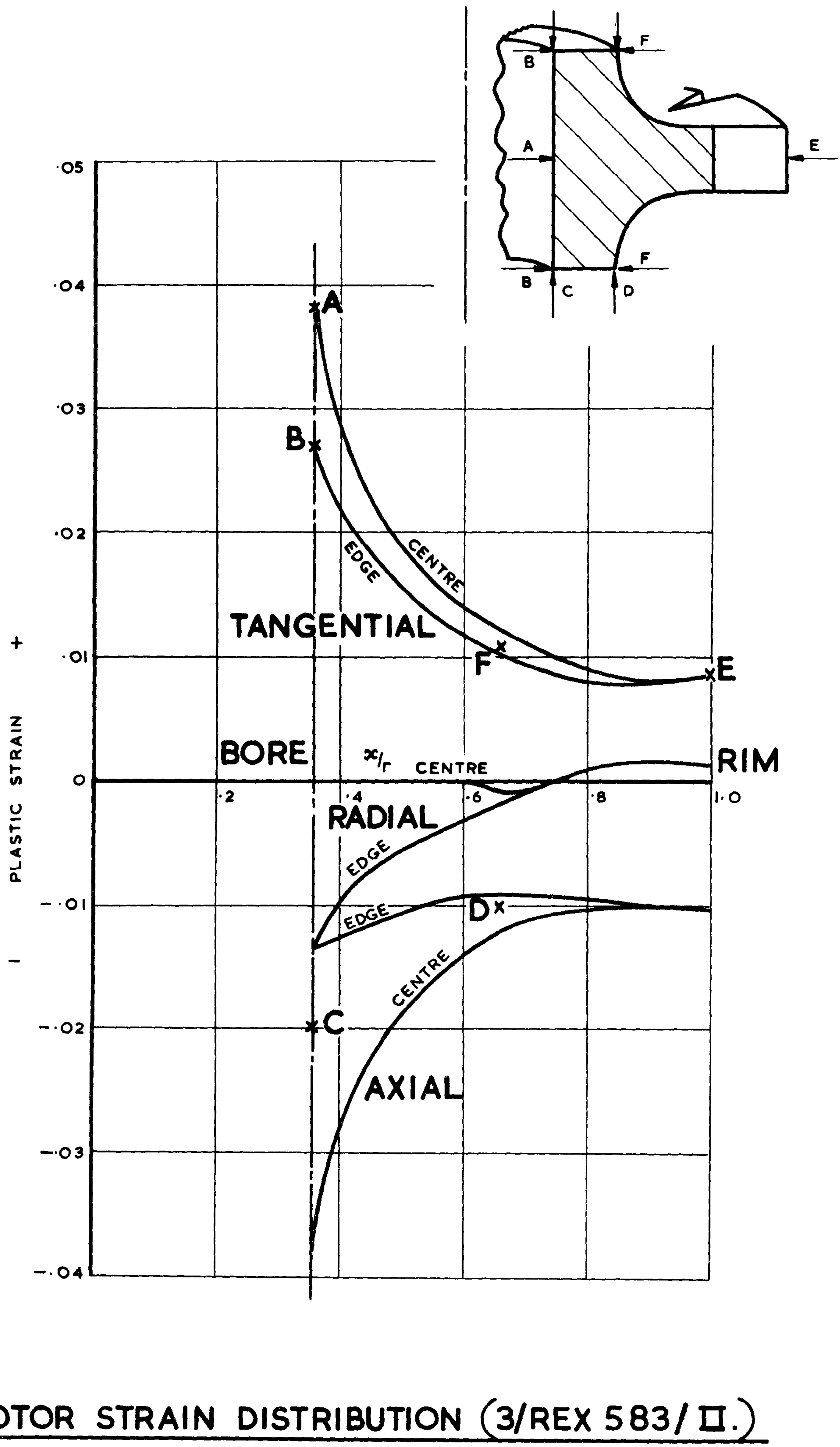

ROTOR STRAIN DISTRIBUTION (3/REX 583/ II.)

FIG. 9

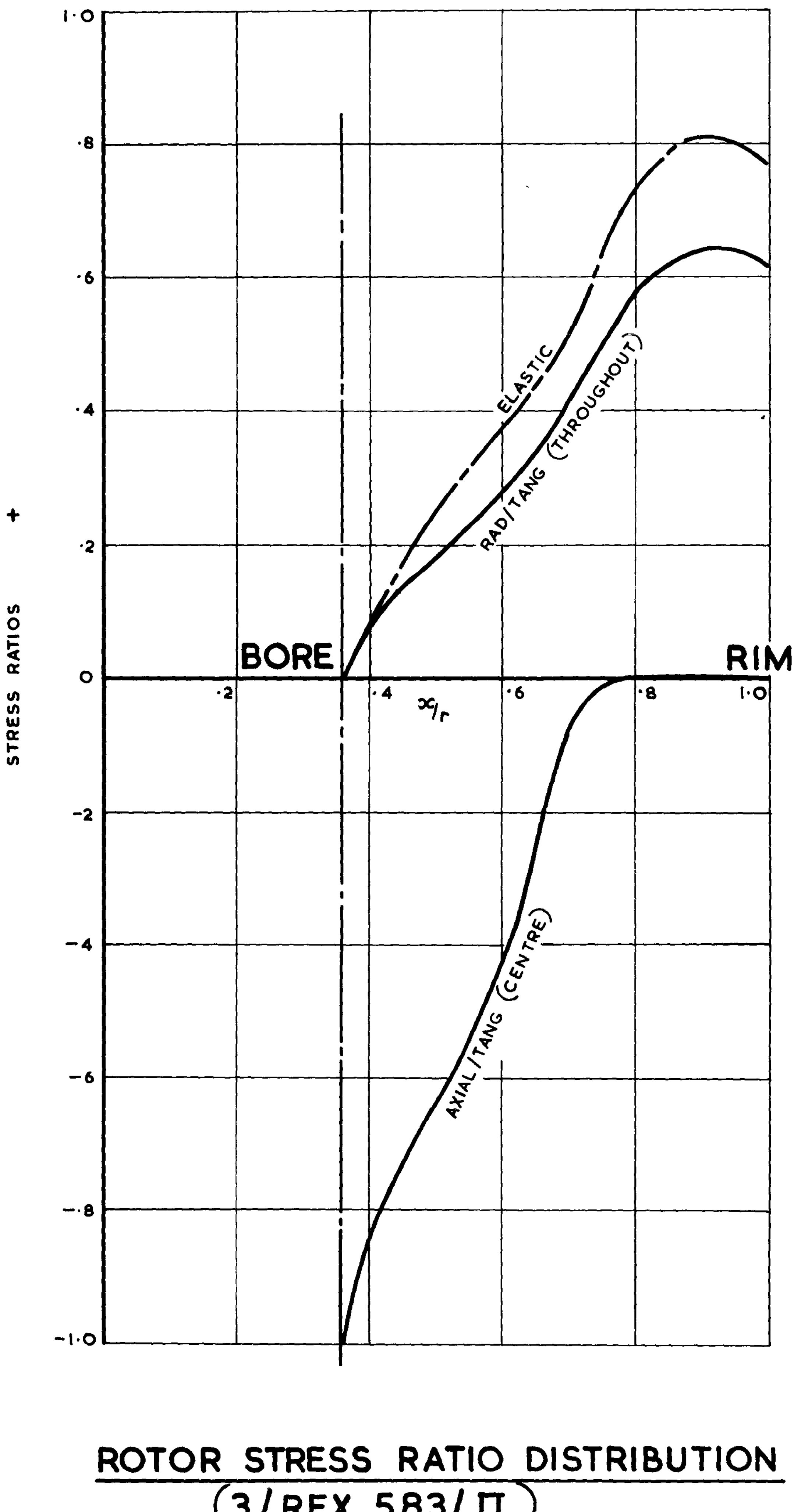

ROTOR STRESS RATIO DISTRIBUTION
(3/REX 583/II.)

FIG. 10(a)

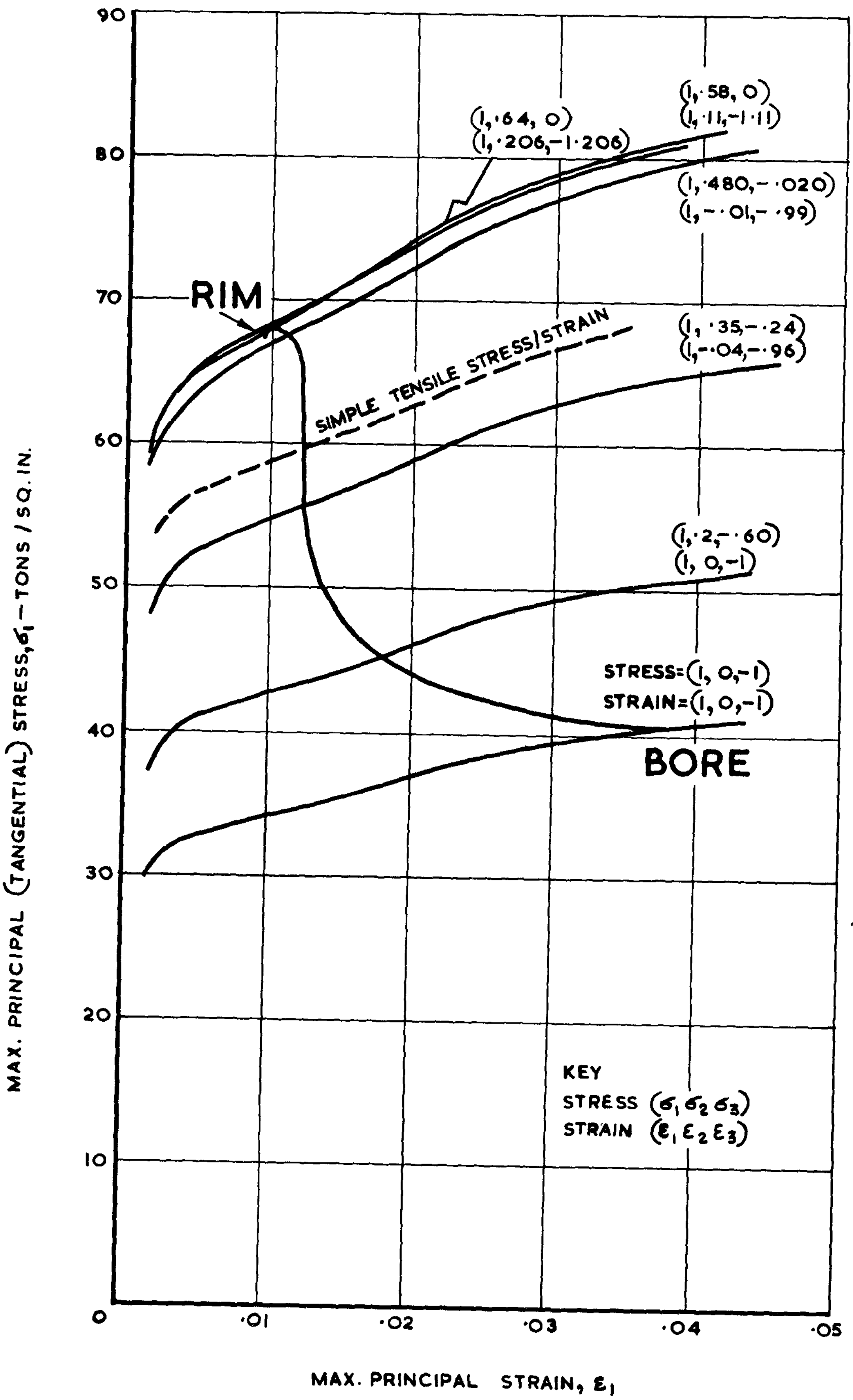

MATERIAL PROPERTIES APPLIED TO CENTRE OF ROTOR (3/REX 583/II)

FIG. 10 (b)

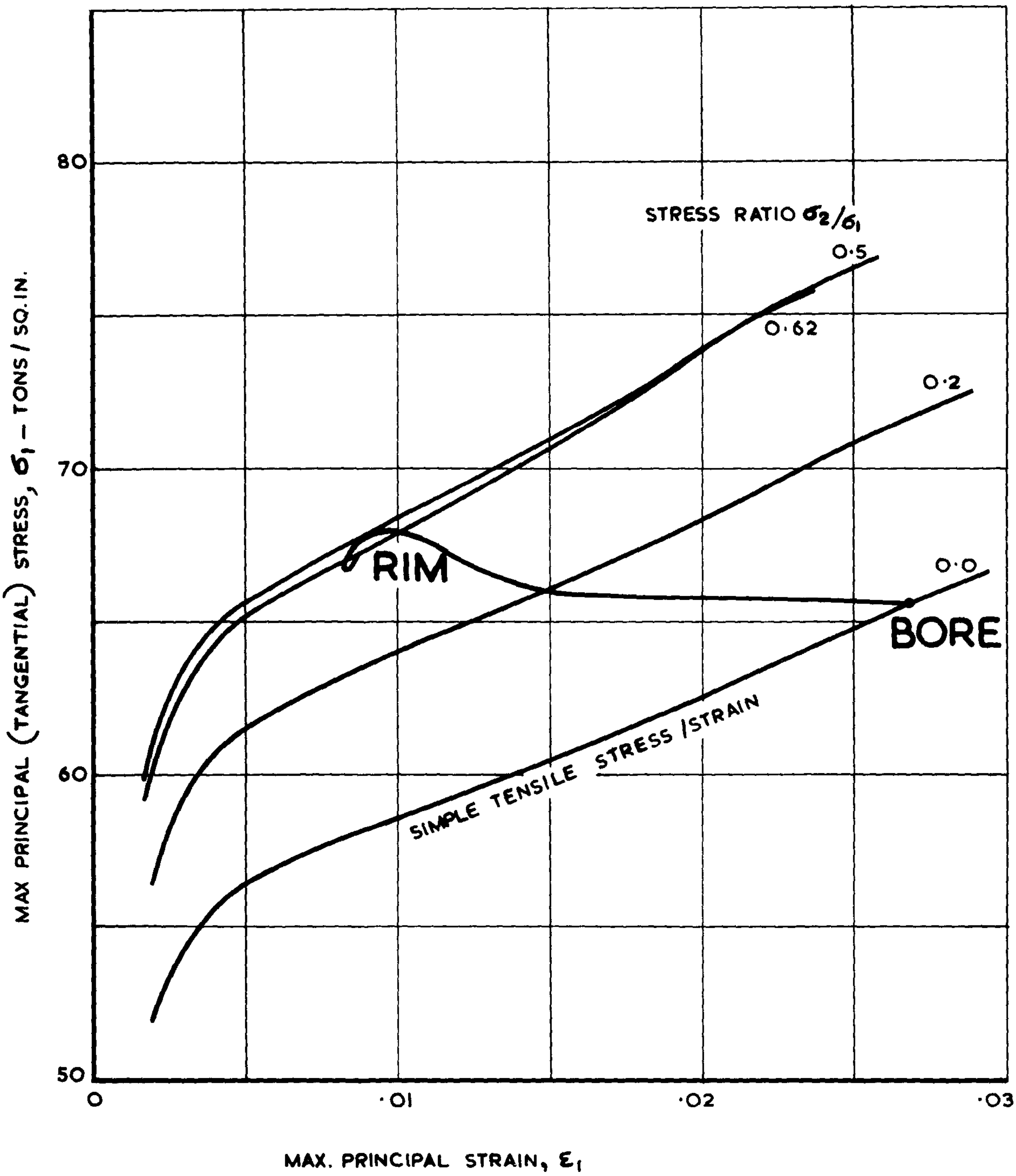

MATERIAL PROPERTIES APPLIED TO EDGE OF ROTOR (3/REX 583/II)

FIG. 11

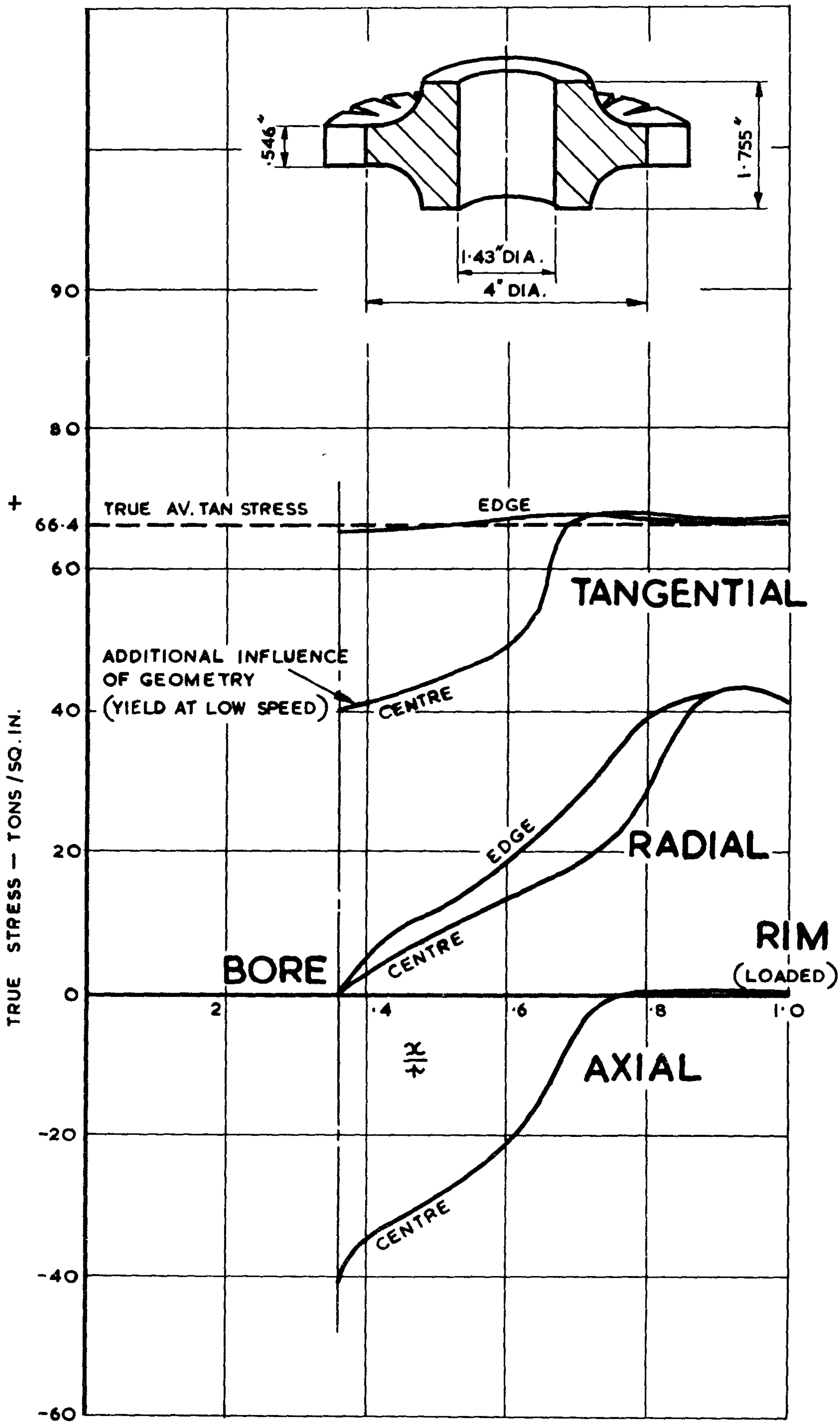

DISTRIBUTION OF STRESS ACROSS ROTOR
(3/REX 583/ II)

FIG. 12

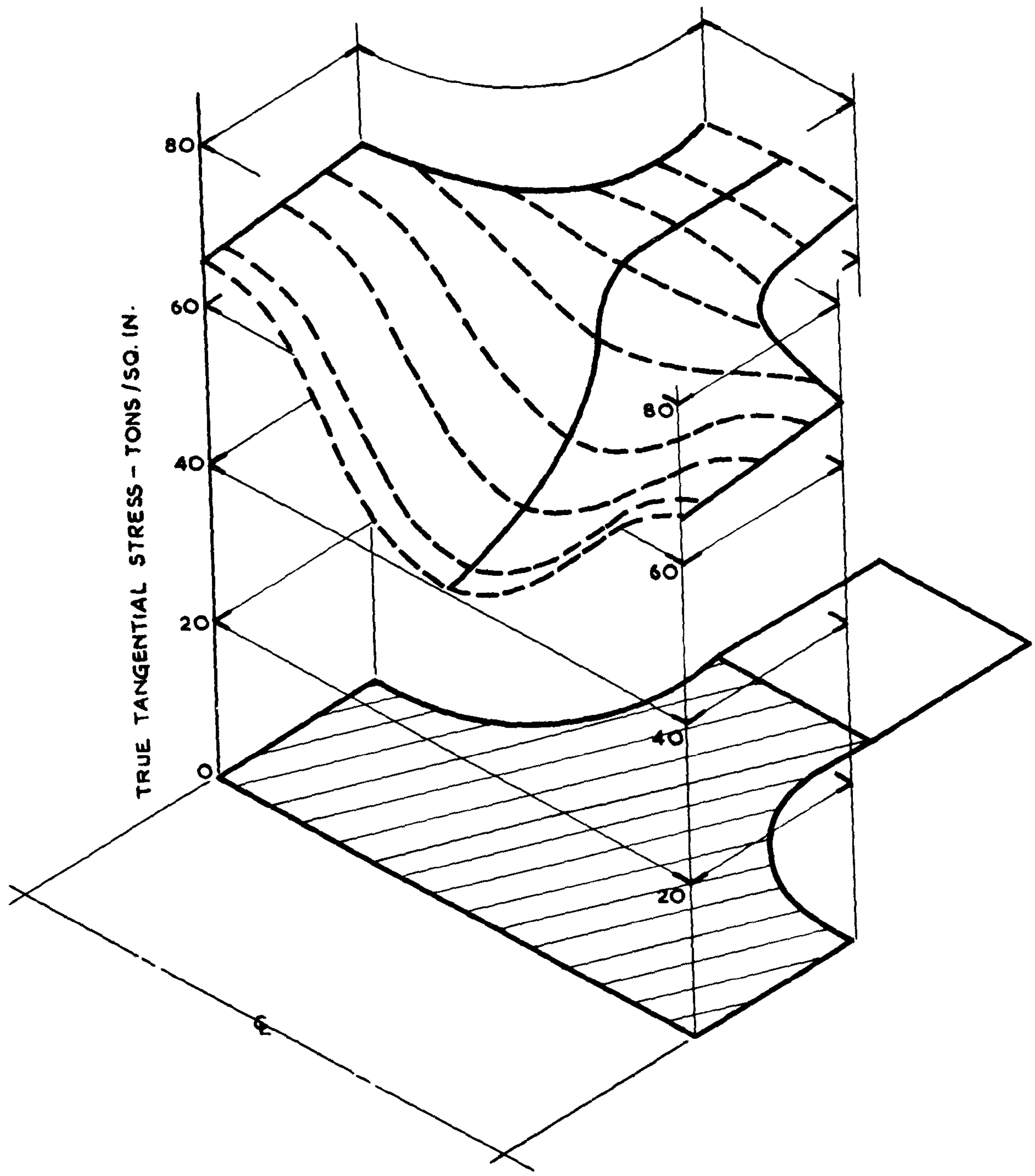

THREE DIMENSIONAL STRESS DISTRIBUTION
IN ROTOR (3/REX 583/ II)

FIG. 13

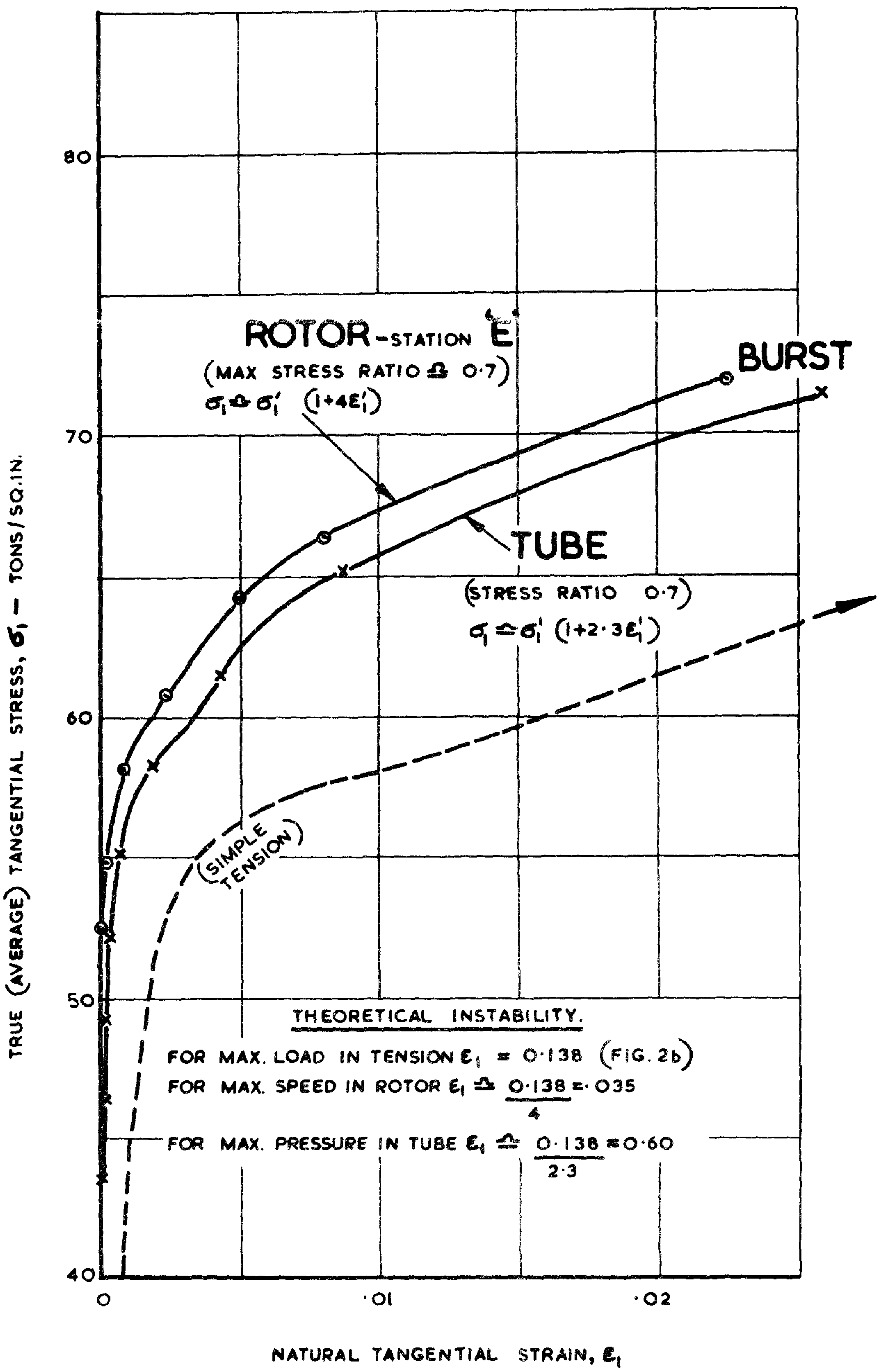

COMPARISON BETWEEN ROTOR AND TUBE STRESS/STRAIN DATA (3/REX/583 II.)

FIG.14.

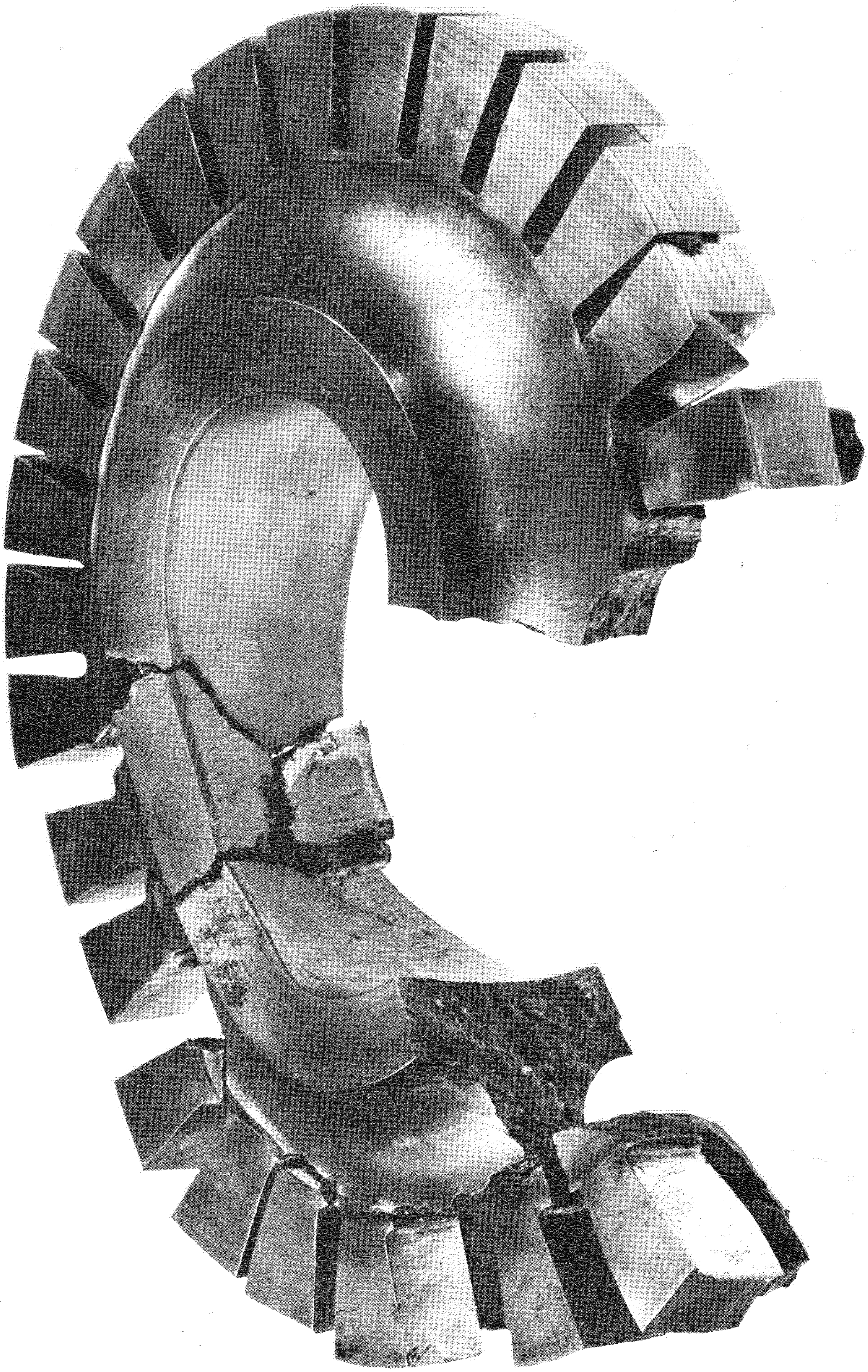

FIG.15.

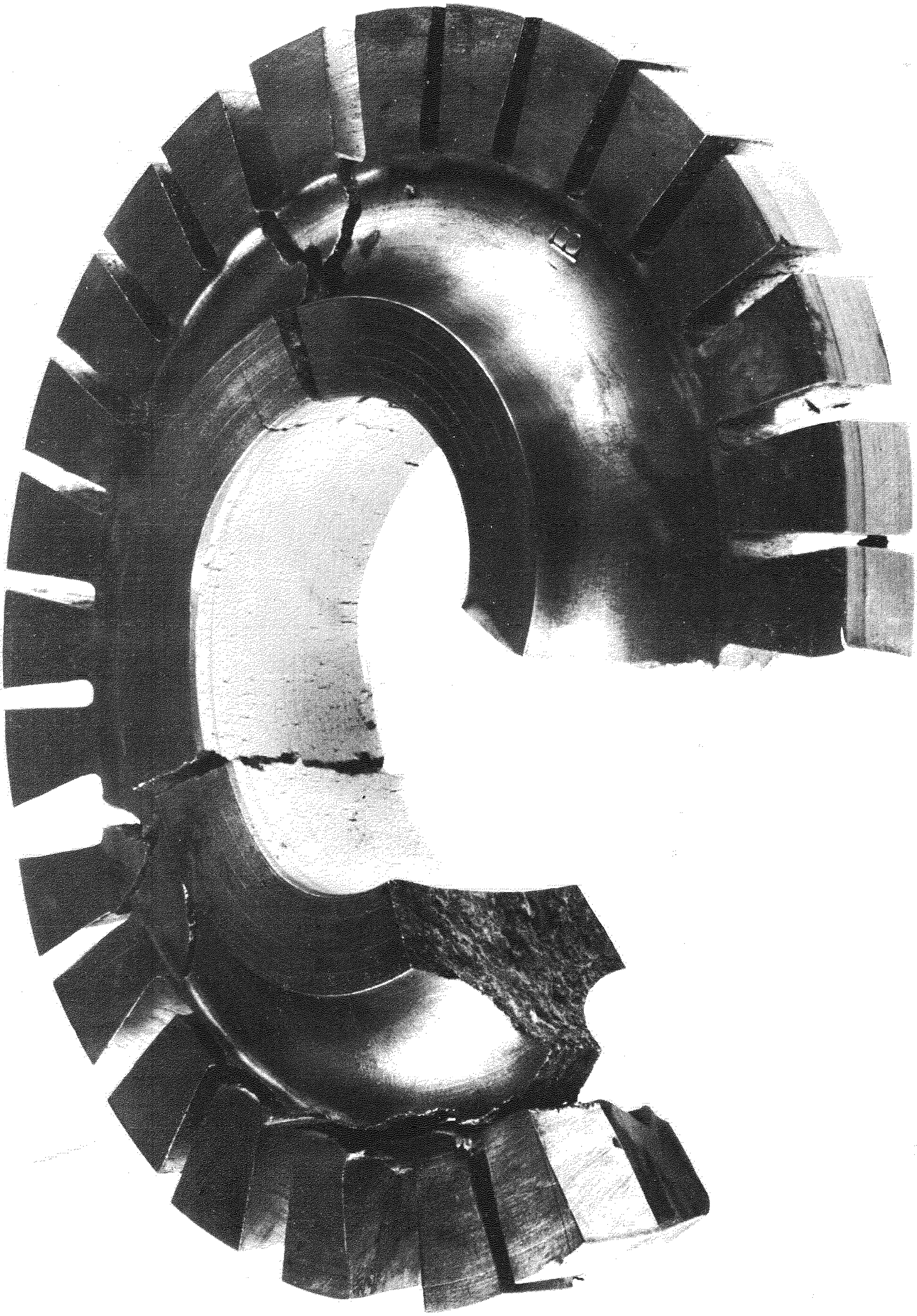

ROTOR FRAGMENTS AFTER BURST TESTS

FIG.16.

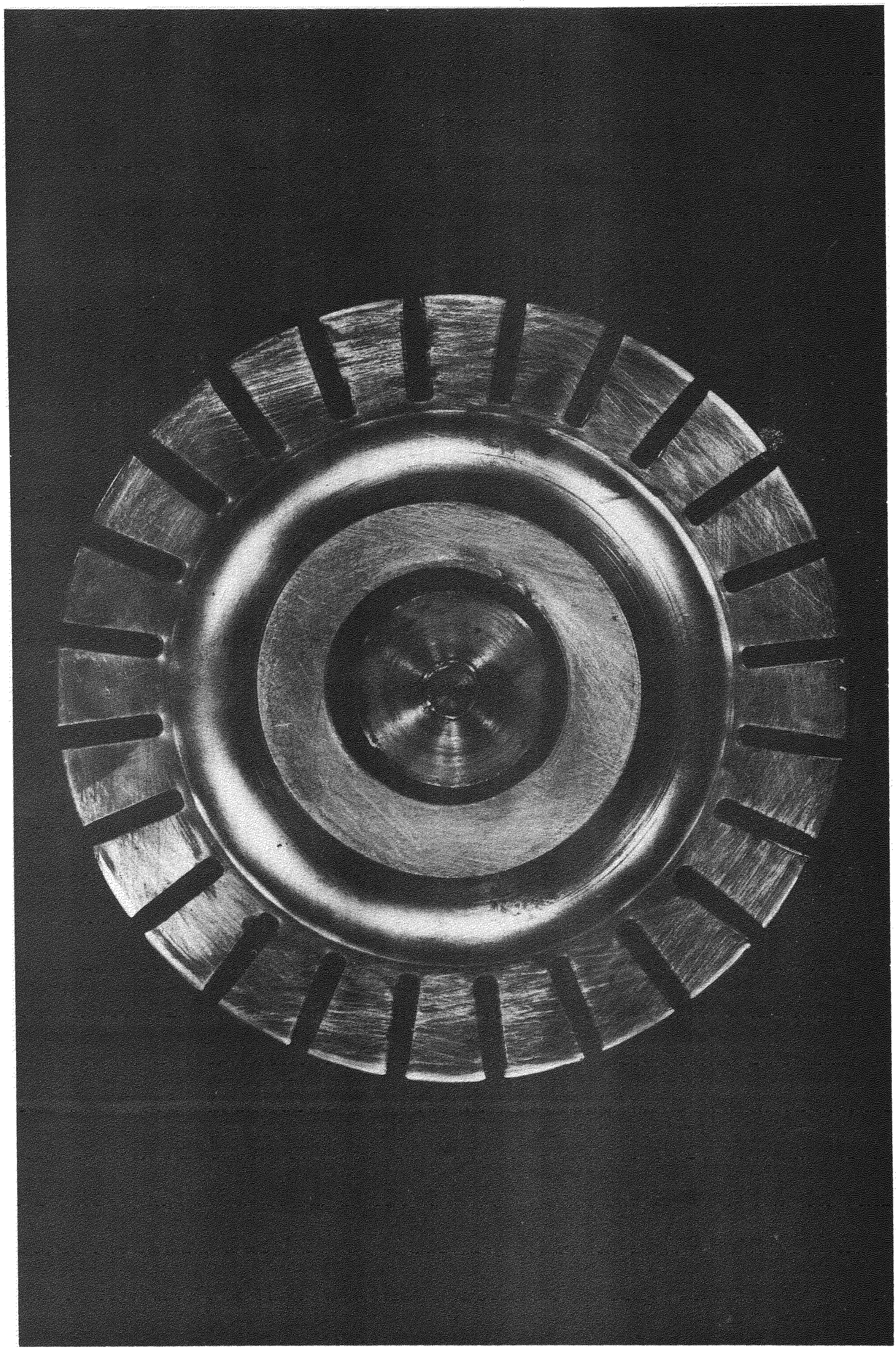

FIG. 17.

1/C1/P1/I

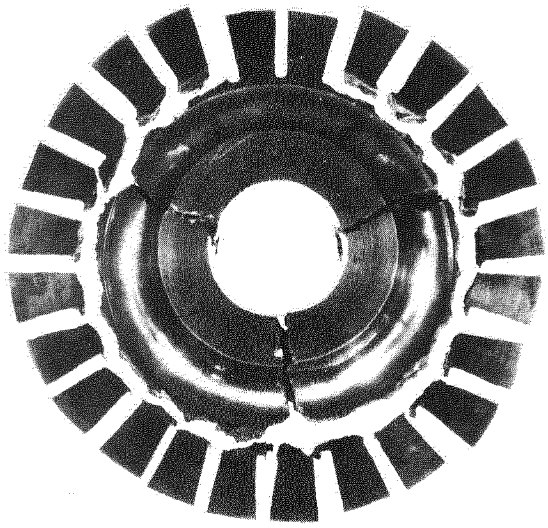

1/C1/P1/II

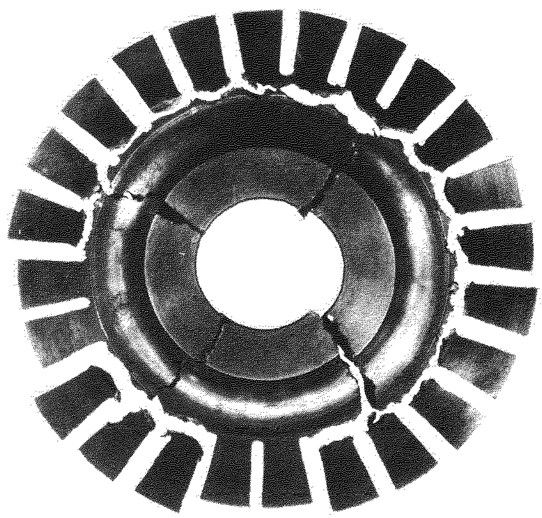

1/C1/P1/III

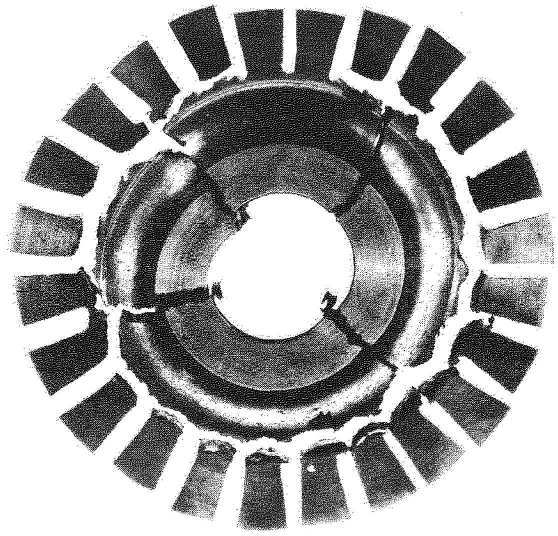

FIG.18.

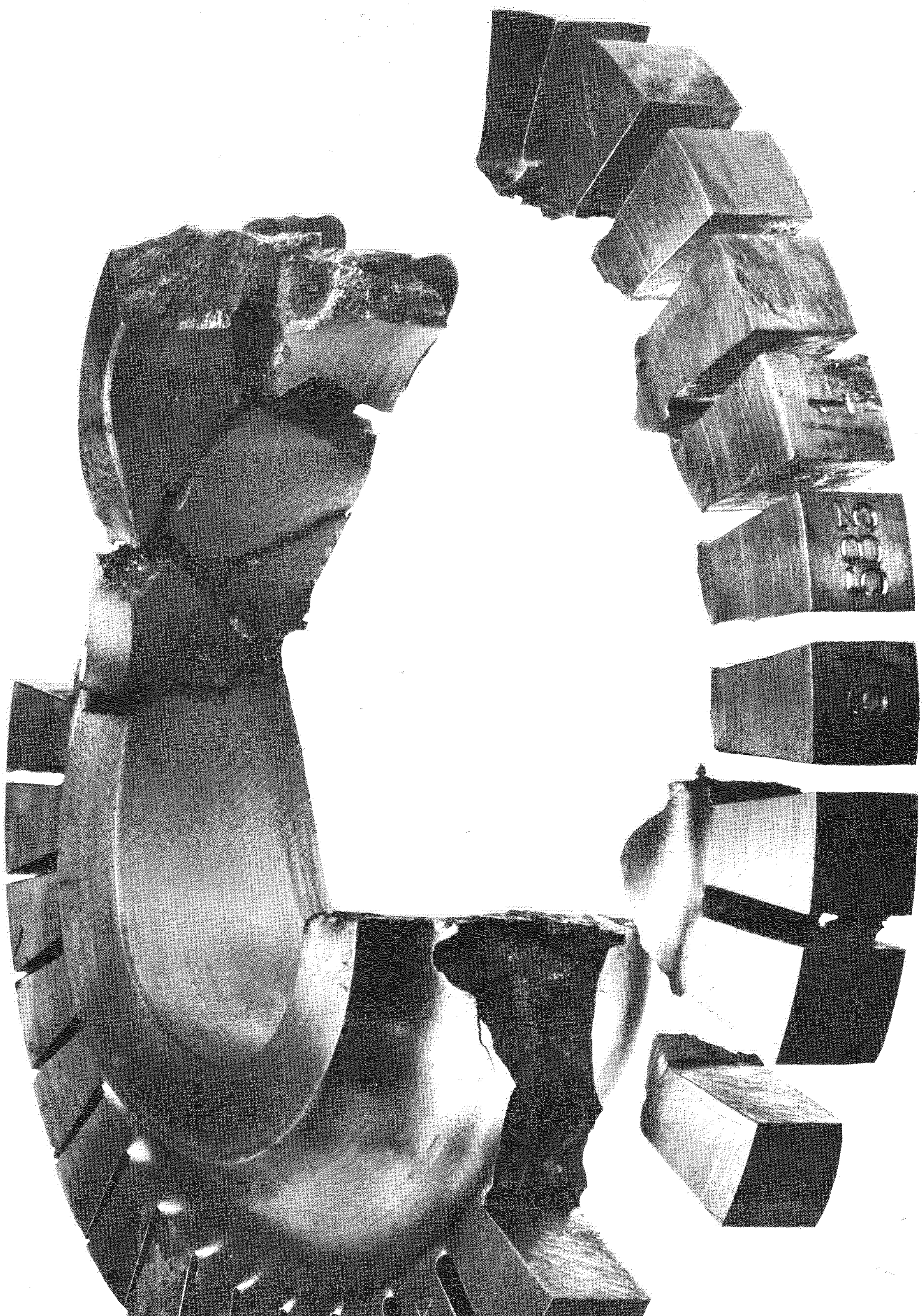

ROTOR FRAGMENTS AFTER BURST TESTS

FIG.19.

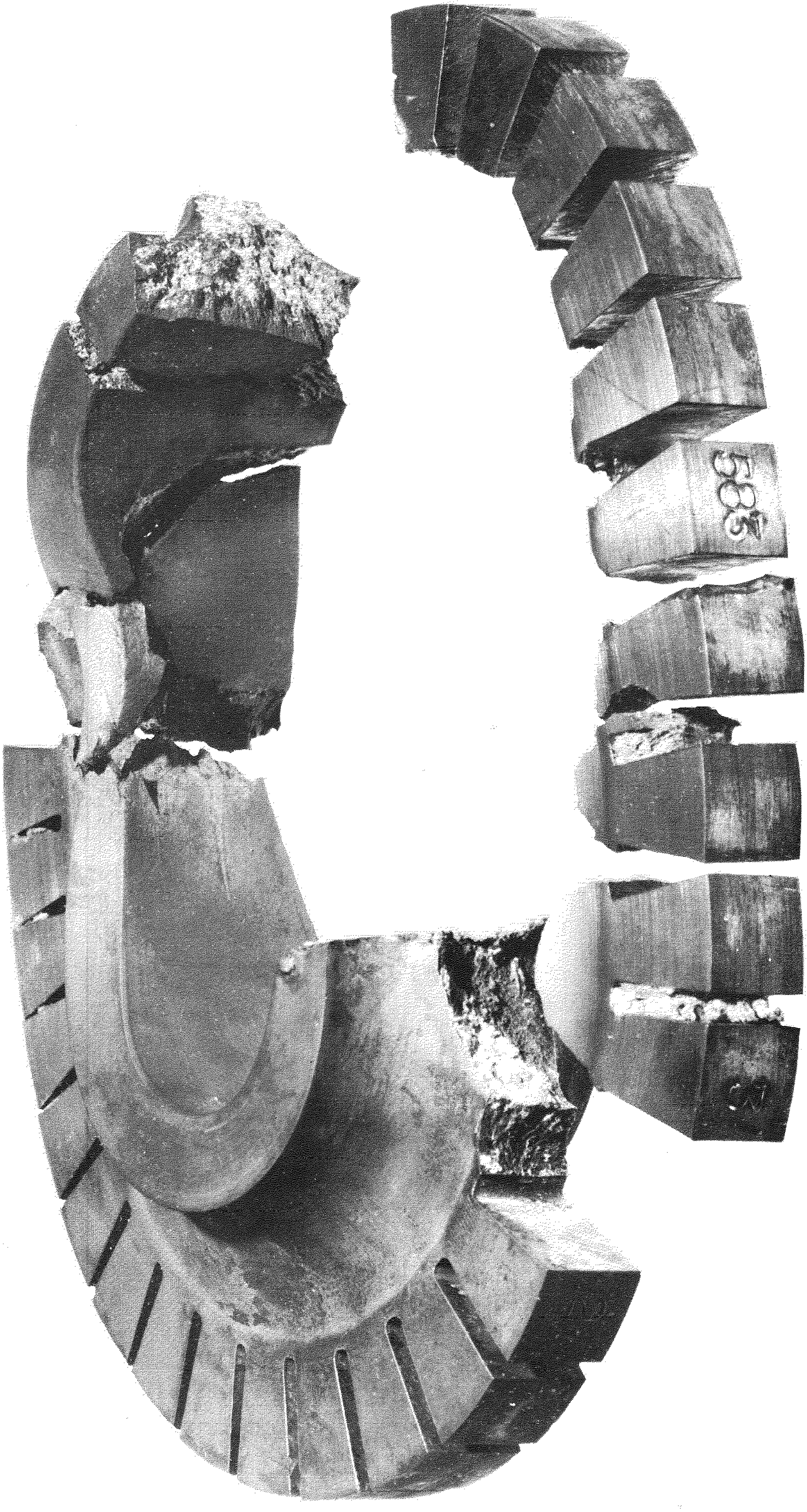

ROTOR FRAGMENTS AFTER BURST TESTS

FIG. 20.

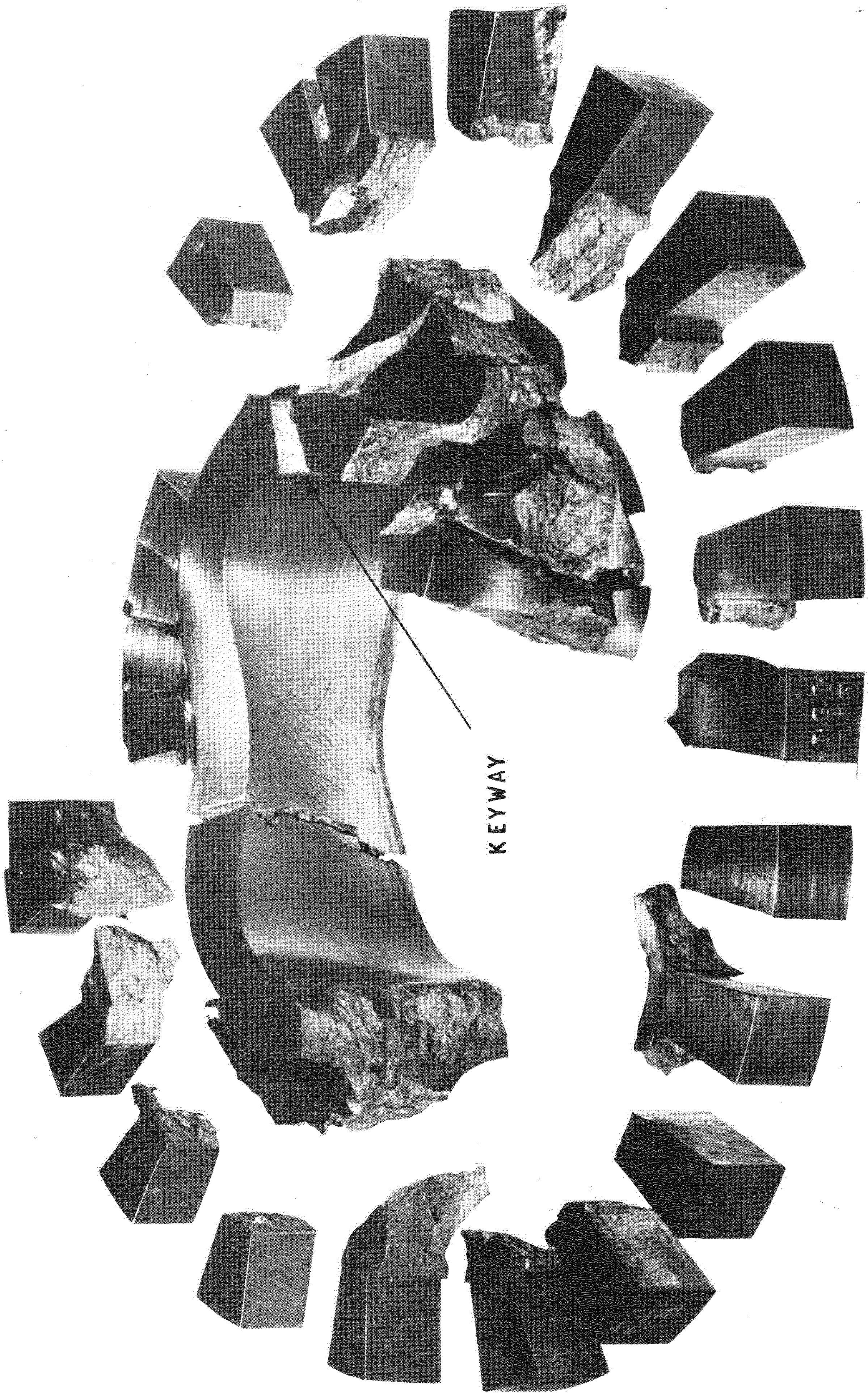

ROTOR FRAGMENTS AFTER BURST TESTS

FIG. 21.

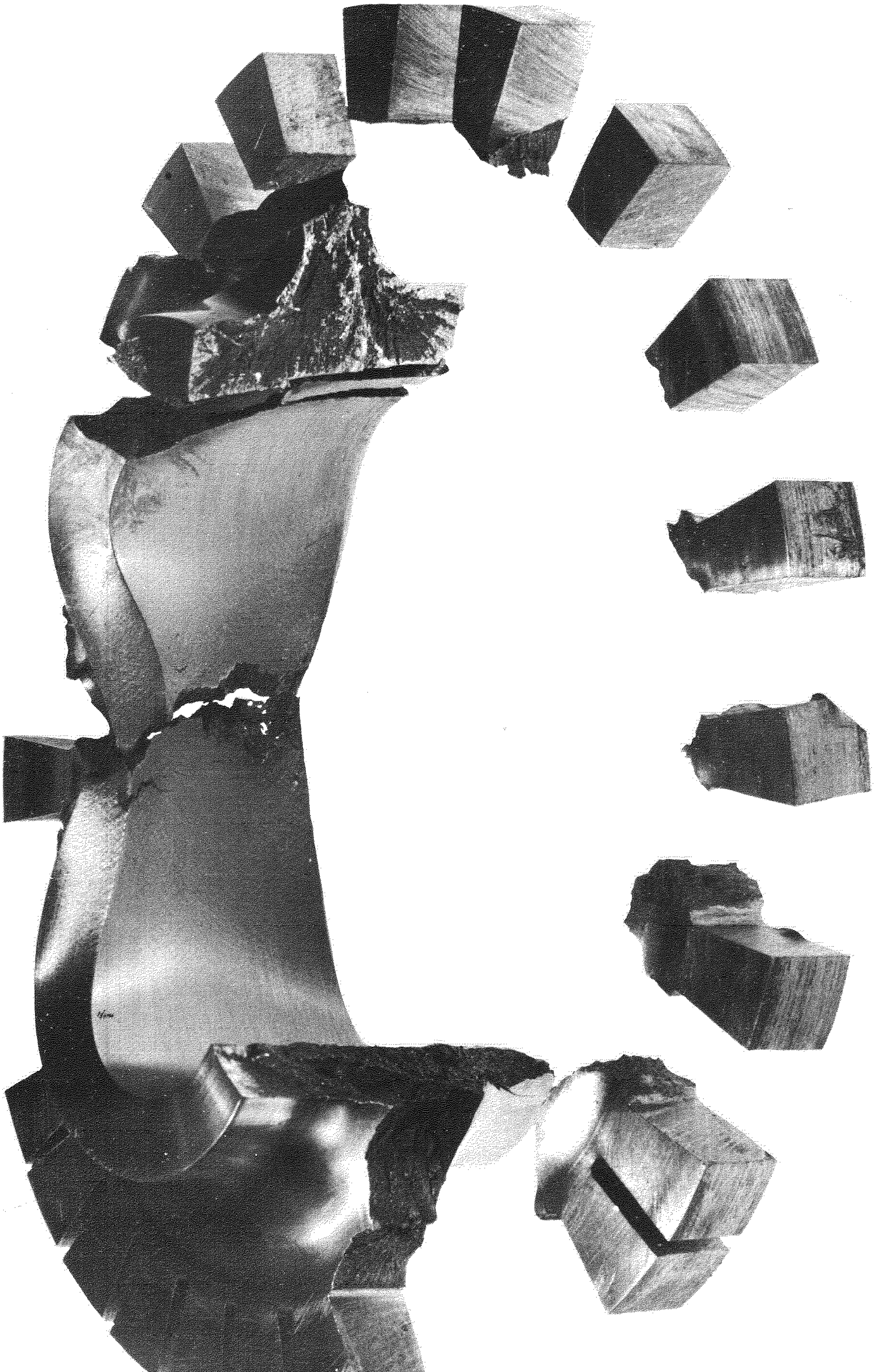

FIG.22.

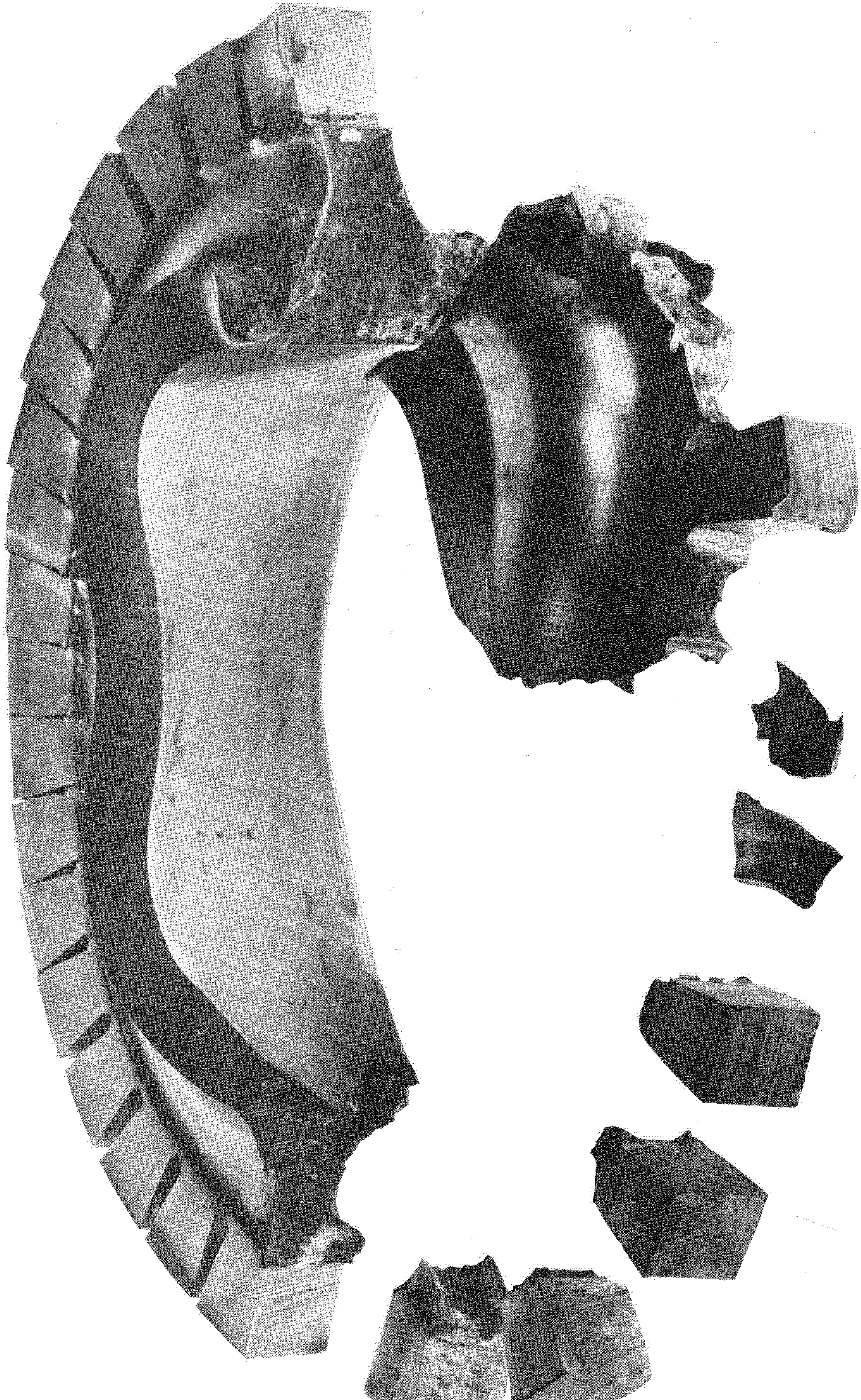

D 28597/1/- 400 7/63 DL

A.R.C. C.P. No. 661 March 1963

531.25-434.3:
620.172

Waldren, N. E. and Ward, D. E.

THE INFLUENCE OF A WIDE HUB ON THE
ROOM TEMPERATURE BURST STRENGTH OF
MODEL STEAM TURBINE ROTORS

A number of model steam turbine rotors in various materials has been spun to burst with the object of studying the influence of increased hub width on rotor strength.

Analysis of results shows that substantial strain in the mid-bore region is the result of a compressive stress which, although improving the ductility of the material, can produce local plastic deformation at low rotor speeds. Failure in the rotors has been caused by a high ratio of biaxial tension near the rim and some changes in design are suggested to reduce this ratio, which severely limits the ductility of the material.

A.R.C. C.P. No. 661 March 1963

531.25-434.3:
620.172

Waldren, N. E. and Ward, D. E.

THE INFLUENCE OF A WIDE HUB ON THE
ROOM TEMPERATURE BURST STRENGTH OF
MODEL STEAM TURBINE ROTORS

A number of model steam turbine rotors in various materials has been spun to burst with the object of studying the influence of increased hub width on rotor strength.

Analysis of results shows that substantial strain in the mid-bore region is the result of a compressive stress which, although improving the ductility of the material, can produce local plastic deformation at low rotor speeds. Failure in the rotors has been caused by a high ratio of biaxial tension near the rim and some changes in design are suggested to reduce this ratio, which severely limits the ductility of the material.

A.R.C. C.P. No. 661 March 1963

531.25-434.3:
620.172

Waldren, N. E. and Ward, D. E.

THE INFLUENCE OF A WIDE HUB ON THE
ROOM TEMPERATURE BURST STRENGTH OF
MODEL STEAM TURBINE ROTORS

A number of model steam turbine rotors in various materials has been spun to burst with the object of studying the influence of increased hub width on rotor strength.

Analysis of results shows that substantial strain in the mid-bore region is the result of a compressive stress which, although improving the ductility of the material, can produce local plastic deformation at low rotor speeds. Failure in the rotors has been caused by a high ratio of biaxial tension near the rim and some changes in design are suggested to reduce this ratio, which severely limits the ductility of the material.

Printed and published by
HER MAJESTY'S STATIONERY OFFICE
To be purchased from
York House, Kingsway, London W.C.2
423 Oxford Street, London W.1
13A Castle Street, Edinburgh 2
109 St. Mary Street, Cardiff
39 King Street, Manchester 2
50 Fairfax Street, Bristol 1
35 Smallbrook, Ringway, Birmingham 5
80 Chichester Street, Belfast 1
or through any bookseller

Printed in England

S.O. Code No. 23-9013-61

C.P. No. 661